2013

Biocomposite Material Evaluation and Processing for Automotive Interior Components

Theresa Lee Sullins
University of Alabama at Birmingham

BIOCOMPOSITE MATERIAL EVALUATION AND PROCESSING FOR AUTOMOTIVE INTERIOR COMPONENTS

by

THERESA L. SULLINS

SELVUM (BRIAN) PILLAY, COMMITTEE CHAIR
ALASTAIR R. KOMUS
LEE G. MORADI
UDAY VAIDYA

A THESIS

Submitted to the graduate faculty of The University of Alabama at Birmingham,
in partial fulfillment of the requirements for the degree of
Master of Science

BIRMINGHAM, ALABAMA

2013

BIOCOMPOSITE MATERIAL EVALUATION AND PROCESSING FOR AUTOMOTIVE INTERIOR COMPONENTS

THERESA L. SULLINS

MATERIALS SCIENCE AND ENGINEERING

ABSTRACT

There is growing demand for materials that are environmentally friendly and sustainable. One of the areas of focus right now is the transportation/automotive field where more energy efficient vehicles are needed to meet growing government regulations and to reduce the negative impacts on global air quality, human health and global climate. Several researchers are focusing on bio-based composites with natural fibers being the prime choice for fiber reinforced composites.

The processing and characterization of 30 wt. % industrial hemp fiber reinforced PP composites for automotive interior components are discussed. The material was compounded by a twin screw and then processed by low shear extrusion and compression molding. The major advantage of this method is the ability to preserve the long fiber length which in turn leads to better mechanical properties. Fiber length and diameter measurements during the various stages of processing show that fiber aspect ratio of approximately 630 was achieved. The effect of chemical treatments and coupling agents are also presented.

5 wt. % MAPP had the best mechanical property results, even after being environmentally conditioned. Compared to neat PP, 30 wt. % hemp fiber with 5 wt. % MAPP had a 91 %, 132 %, 122 % and 297 % increase respectively for flexural strength and modulus and tensile strength and modulus. SEM images of the MAPP specimens illustrated the best interfacial bonding between the fiber-matrix after fiber breakage,

which coincided with the high mechanical properties. MAPP reduced the water uptake by 20 % and had better properties after conditioning than the untreated and NaOH treated specimens. 500 and 1,000 hrs of UV exposure reduced the flexural properties by 30 %, however similar to the hygrothermal test, the MAPP specimens had better properties after being conditioned than the untreated and NaOH unconditioned and conditioned specimens.

After processing and testing evaluation, a male and female tool die for the duct-screen cleaner component was machined for processing 30 wt. % hemp fiber reinforced PP composites with 5 wt. % MAPP. A successful prototype was manufactured that improved the processing method and form and definition of the existing component.

Keywords: biocomposite, industrial hemp fibers, fiber attrition, twin screw compounding, chemical treatment, coupling agent

ACKNOWLEDGMENTS

I have several people I would like to thank for the encouragement, assistance and support that I have received throughout the duration of my study. First, I would like to express my profound gratitude and respect I have for my research advisor, Dr. Selvum (Brian) Pillay. His constant mentorship, motivation, patience and enthusiasm since my undergraduate years enabled me to complete this important milestone in my life. I would also like to thank my other committee members Mr. Alastair Komus, Dr. Lee Moradi and Dr. Uday Vaidya for generously giving their time to offer me valuable comments and insights toward improving my work. Members of the Advanced Plastic and Composites group also deserve my sincerest thanks, their friendship and assistance have meant more to me than I could ever express.

I would like to thank Composites Innovation Centre, Canada for without whom I would not have this research and co-funding of my research. MacDon Industries for the component part. In addition, I would like to mention that this research was partially supported by the National Science Foundation (NSF) and Department of Energy (DOE) Graduate Automotive Technology Education (GATE) program.

I would especially like to thank my beloved father and mother for all their unconditional love, support and strength. Without their guidance, I would not be the person I am today. My little sister that has supported and encouraged me in all my endeavors. And most of all, my loving, supportive, encouraging and patient husband Nick

whose faithful support is so appreciated. Words cannot describe how grateful I am to everyone in my life. Thank you.

TABLE OF CONTENTS

Page

LIST OF TABLES

LIST OF FIGURES

Figure *Page*

INTRODUCTION

Composite Challenges in the Automotive Industry

The volume and number of applications using fiber reinforced composite materials have grown steadily and have become one of the dominant emerging materials. Fiber reinforced composites have diverse applications used in several fields: automotive, construction, marine, electronic components, consumer products, appliances and aerospace to name a few. The automotive field is the leading sector that consists of 31 % usage of fiber reinforced composites [1]. Compared to conventional materials such as metals, composite materials have the advantage due to their ability to meet diverse design requirements with significant weight savings as well as comparable or better mechanical properties in the automotive industry. With the drive to make composites economically attractive, several innovative manufacturing techniques and materials have been developed and utilized. Composites are already proven as weight-saving materials; however, making them cost effective, lower carbon footprint and recyclable still prove to be a challenge.

In recent years, there has been increased awareness of developing and utilizing materials for the transportation/automotive field that are eco-friendly and sustainable. The automotive field in the United States (U.S.) is responsible for about 10 % of the world's carbon dioxide (CO_2) emissions from fuel combustion [2]. Worldwide fuel consumption averages 1,800 kg of oil equivalent per person per year with North America

using over 3,000 billion kilograms of oil equivalent, which is twice the consumption rate of that in Europe [3].

The U.S. is responsible for nearly one-third (534 million metric tons) of all domestic energy and total emissions including: carbon dioxide (CO_2), carbon monoxide (CO), nitrogen oxides (NO_x), sulfur dioxide (SO_2) and volatile organic compounds (VOC) [4]. Transportation in the U.S. accounts for nearly 50 % of NO_x's, 40 % VOC's and is responsible for 80 % of the nation's CO_2 emissions [5]. Carbon emissions are projected to continually increase by an average of 1.3 % a year through 2020; global vehicle usage will increase by a factor of 3-5 by 2050 [6, 7].

The most common fiber reinforced polymer composite used in the automotive industry is glass fibers due to its low cost and high properties. However, they have several disadvantages such as high abrasive wear on processing machinery and health risks among people who work around it. Glass fibers can cause skin and respiratory irritation in the upper respiratory tract due to the large size of the fibers. The National Institute for Occupational Safety and Health (NIOSH) recommends exposure to glass fibers be limited to 3 fibers/cm^3 having a diameter ≤ 3 μm and a length ≥ 10 μm [8]. When a kilogram of glass fiber is melted during processing, 1 kilogram of CO_2 is emitted into the atmosphere in addition to the NO_x, SO_2 and VOC [9]. Glass fibers as well as other synthetic fibers are difficult to dispose of at the end of their 'lifetimes', which poses an issue with recycling. This problem has become a major issue with landfill sites filling up at a faster pace which leads to global warming [10]. According to a report from PR Newswire (2011), fiberglass global output will reach a total of 4.88 million tons by 2012

and will continue to increase at an annual rate of 7.2 %, which will approximate 400k tons of waste generated from fiber reinforced plastic composites [11].

Motivation

Government regulations have been implemented throughout several countries due to the increase in fuel consumption, carbon emissions and landfills. Europe has been the leading innovator in utilizing alternative materials, especially the use of natural fibers, for automotive applications due to government support, environmental regulations and customer acceptance [12]. The European Union (EU) Council of Ministers approved the end-of-life-vehicle directive in July 2002 for the use of natural fibers in the automotive industry. This directive states, "From 2015 onwards, all new vehicles should be 85 % reusable and recyclable by weight, 10 % can be used for energy recovery and only 5 % can be disposed of in landfills" [13]. This initiative can be seen in a global scale not just in the European countries.

With Europe's initiative in becoming more eco-friendly, North America has implemented their own strategy. In 1975, U.S. Congress first enacted the Corporate Average Fuel Economy (CAFÉ) standards to improve the average fuel economy and reduce the weight of vehicles [14]. However, the CAFÉ standards have not been a priority until recently. In 2009, President Barack Obama established a more stringent CAFÉ standard due to issues concerning environment and global warming. It is expected by 2016 that automotive companies must achieve a combined average fuel-economy standard of 35.5 mpg (39 mpg for cars and 30 mpg for trucks and SUVs), which is a 40 % improvement over current standards [15].

More energy efficient vehicles are needed to meet growing government regulations and to reduce the negative impacts on global air quality, human health and global climate. One of the ways to achieve efficiency in the automotive world is to reduce the structural weight with new structural designs and alternative, sustainable materials. If 10 % of weight is reduced from a vehicle's total weight, the fuel economy should improve by 7 % and every kilogram of reduced weight will reduce 20 kilograms of CO_2 [16]. Several researchers are focusing on recyclable composites with natural fibers the prime choice for fiber reinforced composites. The use of natural fibers as reinforcement or fillers yields lower carbon footprint and environmentally sustainable materials with mechanical properties suitable for the automotive industry as well as the transportation and construction industries [17].

Natural fibers have become increasingly suitable alternatives to synthetic fibers and are receiving increased attention from both academic and industry due to its low cost and low density. Natural fibers, when used with thermoplastic resins, offer great advantages such as biodegradability, recyclability, low density, low abrasiveness, enhanced energy recovery, high strength to weight ratio and non-toxicity [18-20]. These renewable natural fibers offer the potential to replace conventional synthetic fibers in most automotive components with the desirable specific properties.

In 2005, Europe utilized over 30,000 tons of natural fibers annually, excluding wood, in the automotive industry. 50,000 tons of natural fibers are expected to be used by 2015 with at least 10-20 % being European hemp fibers [21]. Natural fiber reinforced composites already have been utilized in several automotive components as shown in Table 1.

Table 1

Natural fiber uses in automotive components [22, 23]

Manufacturers	Model(s)	Application(s)
Audi	TT, A2, A3 and A4 Avant	Seat back
		Side and back door panels
		Rear Storage Panel
BMW	3, 5 and 7 Series	Door inserts and panels
		Headliner panel
		Boot lining
Cadillac	DeVille	Seatback
Chevrolet	Impala	Trim
		Rear Shelf
Citroen	C4	Door inserts
Daimler Chrysler	A, C, E and S Klasse	Dashboard
		Business table
		Column cover
Ford	Flex and Focus	B-column cover
		Parcel tray
		Interior storage bin
		Loadfloor
GMC	Terrain	Acoustic insulator
		Ceiling liner
Honda	Pilot	Floor area parts
Lexus	CT200h	Luggage compartment
		Floor mats
Mazda	5 Hydrogen RE Hybrid	Console
		Seat fabric
Mercedes-Benz	A and C Class	Engine and transmission cover
		Underbody panels
Toyota	Prius	Instrument panel
		Air conditioning vent
Volkswagen	Golf A4 and Passat Variant	Seat back
		Rear flap lining
Volvo	C70 and V70	Door inserts
		Parcel tray

Research Objectives

The aim of this work is to maintain critical fiber length by optimizing the extrusion-compression molding process to improve mechanical and environmental properties of hemp fiber reinforced polypropylene composites for automotive components. Fiber chemical treatments and coupling agents are understood from previous research to enhance the interfacial bonding of the fiber and matrix.

The objectives of the proposed research are as follows:

- Use a design of experiment (DOE) approach for evaluating hemp fiber attrition at each composite manufacturing stage to achieve higher aspect ratio.
- Characterize and evaluate chemical treatments and coupling agents to enhance fiber-matrix bonding and properties.
- Evaluate the performance of hemp fiber reinforced PP composites in consideration of cost and processing time and energy.
- Modify the component design to be compatible with the processing method and design a female-male tool die.
- Manufacture a successful prototype.

LITERATURE REVIEW

Composite Overview

Composites have become an integral part of our day-to-day life and can be found everywhere from human bones to automotive designs. A composite material can be defined as two or more physically/chemically distinct, suitably arranged or distributed phases with an interface separating them that could be manufactured [24]. Composites offer several advantages over traditional metal components such as weight reduction, low cost, wear resistance, design flexibility, corrosion resistance, durability and high strength but also some disadvantages as shown in Table 2.

Table 2

Advantages and disadvantages of composites [25, 26]

Advantages	Disadvantages
• Lightweight • High specific stiffness • High specific strength • Tailored properties (anisotropic) • Low electrical conductivity • Part consolidation leading to lower overall system cost • Easily bondable • Good fatigue resistance • Easily moldable to complex (net) shapes, design flexibility • Good damping • Internal energy storage and release • Crash worthiness • Low thermal expansion	• Damage susceptibility • Lack of well-proven design rules • Long development time • Manufacturing difficulties • Fasteners • Low ductility (joints inefficient, stress risers more critical than in metals) • Solvent/moisture attack • Temperature limits • Cost of material (dependent on application and process)

Composite Classification

Composites for this research can be classified based on their matrix and fiber. Fiber reinforced composites are the most widely used composite materials in the aerospace and automotive industries. The matrix is a continuous phase that transmits externally applied loads to the reinforcement, protects the reinforcement from external mechanical and environmental damage and gives shape to the structure. Fibers act as a reinforcement to provide strength, stiffness and other mechanical properties in composites.

Matrix

The matrix can be broadly classified into three groups: polymer matrix composite (PMC), metal matrix composite (MMC), and ceramic matrix composite (CMC). PMCs are the most widely used matrix and have established themselves as engineering structural materials. Reinforcing fibers with a polymer matrix can overcome the inadequate mechanical properties of polymers and do not involve high processing pressure and temperature [27].

PMCs can be further sub-divided into two classes as either thermoset or thermoplastic. Thermoset polymers are chemically joined together by the molecular cross-links that connect the entire matrix together forming a three-dimensional network. Thermoset polymers have good thermal stability and chemical resistance; however, they cannot be re-melted or recycled due to the cross-links formed during the polymerization/curing process. They also have limited storage life at room temperature, long fabrication time and low strain-to-failure.

Thermoplastic polymers consist of long, discrete molecules that melt to a viscous liquid at processing temperature then are formed after cooling to an amorphous, semicrystalline material. Thermoplastics offer great promise for the future due to their high impact strength and fracture resistance, ability to be reprocessed and recycled, ease of joining and repair, postformability and shorter fabrication time. Most common thermoplastic resins are polypropylene (PP), polyamides, polystyrene (PS), polyethylene (PE) and polyvinyl chloride (PVC).

Fiber

Fibers can be classified as either continuous or discontinuous fiber (chopped fiber) reinforcements. Continuous fiber reinforced composites are fiber lengths greater than 50 mm that provide the best mechanical properties when loaded longitudinal to the fiber direction and have low properties in the transverse direction. Discontinuous fiber reinforced composites have lower properties than continuous fibers but have the possibility to obtain nearly equal mechanical and physical properties in all directions because of its random, chopped orientation. There has been an increasing amount of discontinuous fiber reinforced composites utilized in engineered applications because of its unique combination of properties that are more economical than competing materials and ability to be adapted to mass production [28]. Discontinuous fibers can be further divided into two groups based on the fiber length, short and long fiber, in thermoplastic processing applications. Short fibers are generally less than 4 mm long, and long fiber lengths are between 8 to 50 mm [29, 30]. In this research, long fibers are of interest and

will be further discussed in the following section, Factors Affecting Composite Properties.

Interface vs. Interphase

In fiber reinforced composites, the fiber and matrix both retain their physical and chemical identities producing a combination of properties that cannot be achieved with either constituents acting alone, due to the interface between the two constituents. According to Metcalf, "An interface is the region of significantly changed chemical composition that constitutes the bond between the matrix and reinforcement" [31]. The interface boundary maintains the bond in between the fiber and matrix for the transfer of loads and has unique physical and mechanical properties compared to the fiber and matrix. In contrast, the interphase exists from some point in the fiber through the actual interface into the matrix and has physical and mechanical properties between those of the fiber and matrix. Therefore, the interface definition can be used for the interphase definition.

The interface plays a key role in transferring the stress from the matrix to the fiber, stability of the structure and fracture behavior in a composite material. The interfacial bonding/adhesion bonds the fiber and matrix through mechanical interlocking, chemical bonding, electrostatic bonding and/or interdiffusion bonding that determines the amount of stress that is transferred from matrix to fiber and reinforcement efficiency of the fibers in the matrix [32]. A weak interface results in low strength and stiffness but high fracture resistance; a strong interface produces high strength and stiffness but low fracture resistance [33].

Processing

Injection molding is the most common and widely used thermoplastic method for processing automotive parts. The injection molding machine closely resembles an extruder except it sequentially plasticizes the thermoplastic pellets in a heated barrel, delivers the homogenous melt to the machine nozzle and acts as a ram to quickly inject the melt into a closed mold. Short fibers used for injection molding have a relatively low fiber fraction but have enough fiber content to act as a sufficient reinforcement [13]. Injection molding can produce intricate shapes in high volumes at high production rates.

Injection molding possesses a few issues that affect the mechanical properties of the composites. Holbery et al. reported that one of the challenges posed by injection molding is to produce pellets of a consistent quality, especially when using natural fiber in direct long fiber thermoplastics [12]. Ishida et al. reported that extensive fiber damage occurs from injection molding from the high shear, intensive mixing and narrow gates of the process [34]. Short fibers may act as filler instead of as reinforcement in composite applications due to fiber attrition.

The extrusion process is one of the most effective methods of compounding short and/or long reinforcing fiber reinforced thermoplastic polymers in pellet or powder form. Both fiber and polymer are combined and drawn into a heated extrusion either utilizing a single screw or twin screw extrusion to produce a homogenous material at constant temperature and pressure. Single screw extruders melt the polymer, mix with the short/long reinforcing fibers, devolatilize unwanted gases from the composite melt and then the composite forms into the die shape [35]. The twin screw extruder has a similar processing method; however, it can control the melt flow mechanism that can provide for

various types of mixing and compounding down to near-molecular level with two co-rotating screws. This compounding method can achieve excellent fiber distribution and high aspect ratio within the polymer matrix and may be chopped into pellets that can easily be injection molded into more complex shapes or reintroduced to the single screw extrusion-compression molding process [36]. The extrusion method can produce excellent mechanical properties by optimizing the barrel length, temperature profile, screw configuration and screw speed [13]. Incorrect setup can result in poor dispersion, poor wetting of fibers, and fiber degradation.

Factors Affecting Composite Properties

In fiber reinforced composites, maximum properties can be achieved by selecting a suitable fiber and by controlling various parameters such as fiber volume fraction, fiber aspect ratio and dispersion and orientation of fibers. Due to the variation in fiber length distribution in short and long fibers and processing variability, the three factors affecting composite properties cannot be controlled precisely during manufacturing [37]. Each of these factors affecting composite properties is described in detail below.

Fiber Volume Fraction

Fiber volume fraction (V_f) is one of the most important factors controlling the mechanical properties of composites, especially the strength and stiffness. There are two possible failure regimes depending on whether the fiber volume fraction is above or below the minimum value (V_{min}). If $V_f < V_{min}$, the failure regime is in the matrix. The polymer matrix is designed to carry the applied load after fiber failure resulting in a stress

increase in the matrix. The composite itself does not fail, and the failed fibers can be regarded as holes in the polymer matrix since the fibers carry no load. If $V_f > V_{min}$, the failure occurs when the fiber fails. The polymer matrix is unable to support the additional load that is transferred from the fiber to the matrix. The failure of the fiber leads to the failure of the whole composite. Thus, a certain amount of fibers is necessary to ensure that the composite strength is increased over that of the matrix strength alone, which is called the critical fiber volume fraction (V_{crit}). At very high fiber volume fractions, the strength of the composites starts to decrease due to insufficient wetting of the fibers [38, 39]. Nishino et al. found that composite strength increased with an increase in fiber volume fraction until 70 % fiber volume where it started to show a reduction in strength [40].

Fiber Aspect Ratio

Fiber aspect ratio (length/diameter) is another critical parameter that affects the mechanical properties of composite materials. The critical fiber aspect ratio of a composite is the minimum fiber aspect ratio in which the maximum allowable fiber stress can be achieved for a given load, which can be calculated using the following equation:

$$\frac{l_c}{d} = \frac{\sigma_f}{2\tau_i} \tag{1}$$

where l_c is the critical fiber length, d is the fiber diameter, σ_f is the fiber tensile strength and τ_i is the interfacial shear strength. Critical fiber length is the minimum length of the fiber required for the stress to reach the fracture stress of the fiber. Shorter fiber lengths

will not carry the maximum load that longer fiber lengths are capable of supporting. Short fiber thermoplastics (SFTs) have an aspect ratio of 100-200 after processing [41]. Longer fiber thermoplastics (LFTs) have a greater proportion of the fiber that can be fully stressed which contributes to the composite strength and have higher aspect ratios than SFTs. The use of LFTs has been steadily growing, approximately 30 % per year, in the plastics industry due to the high aspect ratio and resulting properties [42].

The average fiber length is important to retain in processing due to fiber attrition. Long fibers are more desirable than short fibers to maintain a high aspect ratio. However, the processability of the composite will decrease as fiber length increases due to fiber entanglement and poor fiber dispersion and wetting.

Fiber Orientation

Fiber orientation is another important factor that influences the mechanical behavior of composites. Maximum strength in composites occurs if the fibers are aligned and oriented parallel to the direction of the applied load. However, SFTs and LFTs rarely consist of fibers oriented in a single direction due processing. Injection molding creates a phenomenon called fountain flow where the melt is deposited on the mold wall with the fiber alignment parallel to the mold fill direction as shown in Figure 1. Behind the melt front, shear flow dominates and produces fairly uniform levels of fiber alignment; whereas, at the center of the melt the rate of shear is low and transverse fiber alignment is present [43]. The polymer melt in the extrusion process experiences both extensional and shear flow that causes the fibers to align in the flow direction as shown in Figure 2. In

both manufacturing processes, the viscoelastic properties of the polymer matrix, mold design and processing conditions continually change the fiber orientation [44].

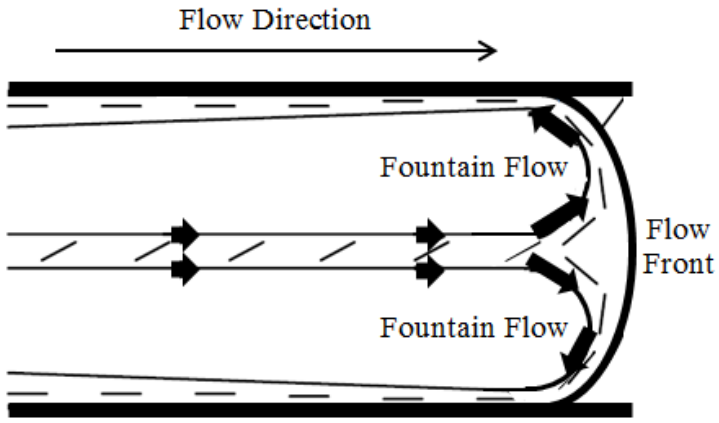

Figure 1. Schematic fiber fountain flow effect during injection molding (adapted and modified from [13]).

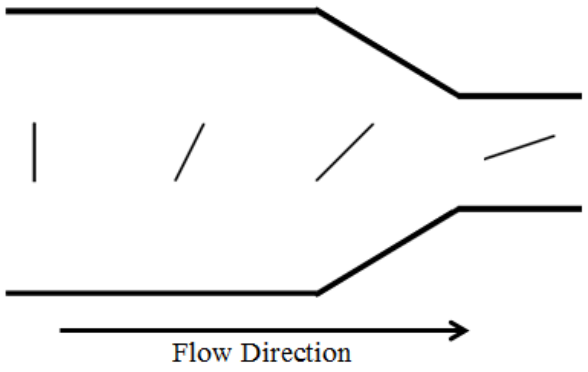

Figure 2. Schematic fiber flow in extrusion process (adapted and modified from [13]).

Natural Fibers

Natural fibers, for this study, are defined as organic fibers that can be derived from plants. The majority of automotive components are plant derived. Plant fibers, often referred to as vegetable fibers, are stronger and stiffer than animal fibers and are also more suitable for composite applications. Plant fibers can be further classified based on their origin into the following categories:

- Bast fibers: Flax, hemp, jute, kenaf, ramie
- Fruit fibers: Coir, oil palm
- Grass/Reed fibers: Bagasse, bamboo, corn, sabai
- Leaf fibers: Abaca, agave, banana, PALF, sisal
- Seed fibers: Cotton, kapok, loofah, milkweed
- Stalk fibers: Barley, maize, oat, rice, rye
- Wood fibers: Softwood, hardwood

Bast fibers are the principal fibers utilized in automotive components. Bast fibers, especially flax and hemp fibers, have been increasingly used as suitable alternatives to glass fibers due to their cost effectiveness, low density and environmentally friendly aspects in composite applications. Bast fibers are rapidly replacing synthetic fibers as reinforcements in automotive interior components such as door trim panels, trunk liners and hood liners, to name a few, due to their comparable specific strength and modulus. The properties of bast fibers and some synthetic fibers are shown in Table 3.

Table 3

Mechanical property comparison of bast fiber vs. synthetic fibers [45-51]

Fiber Type	Density (g/cm^3)	Tensile Strength (GPa)	Young's Modulus (GPa)	Specific Strength ($GPa/(g/cm^3)$)	Specific Modulus ($GPa/(g/cm^3)$)	Elongation at Break (%)
Flax	1.50	0.35-1.04	60.0-80.0	0.20-0.70	18.4	2.70-3.20
Hemp	1.14-1.48	0.55-1.10	50.0-70.0	0.60	26.3-61.4	1.60
Jute	1.30-1.40	0.39-0.77	13.0-26.5	0.3-0.5	10-18.3	1.16-1.5
Kenaf	1.45	0.93	53.0	0.60	36.5	1.60
Ramie	1.50	0.40-0.94	44.0	0.30-0.60	40.9-85.3	1.50
E-glass	2.50	2.00-3.50	70.0	0.80-1.40	28.0	2.50
S-glass	2.50	4.57	86.0	1.80	34.4	2.80
Aramid	1.40	3.00-3.15	63.0-67.0	2.10-2.20	45.0-47.8	3.30-3.70
Carbon	1.40	4.00	230-240	2.86	164-171	1.40-1.80

Composition

Natural fibers consist primarily of cellulose, hemicellulose, pectin and lignin, which make up 80-90 % of the dry material. The rest of the composition of natural fibers consists of minerals, waxes, water-soluble components, extractives and impurities. Even though all bast fibers come from different species and appear different, their chemical compositions are fairly similar. Chemical compositions of some bast fibers are shown in Table 4.

Table 4

Bast fiber chemical composition by mass percentage [52, 53]

Fiber Type	Cellulose	Hemi-cellulose	Lignin	Pectin
Flax	60.0-81.0	14.0-19.0	2.00-3.00	1.80-2.30
Hemp	70.0-78.0	18.0-22.0	4.00-5.00	0.8-0.9
Jute	51.0-78.0	12.0-20.0	5.00-15.0	0.20-4.40
Kenaf	44.0-72.0	19.0-21.0	9.00-19.0	2.00
Ramie	67.0-76.0	13.0-15.0	0.5-1.00	1.9-2.00

Cellulose

Cellulose is the major framework in plant fibers and acts as a reinforcing structure within the plant cell wall. Cellulose is chemically defined as a linear, semicrystalline polysaccharide consisting of β-D-anhydroglucopyranose units bounded with β-(1 → 4) glycosidic linkages, as shown in Figure 3. The cellobiose is the repeating unit in the cellulose chain consisting of two anhydroglucose units. Since the chain ends are different, the cellulose chain has a direction with a non-reducing end with a closed ring structure and reducing end with aliphatic structure and a carbonyl group in equilibrium with cyclic hemiacetals. The formation of the linear crystalline structure is made from the hydrogen bonds formed by the glucose monomers bonded with both its own chain (intramolecular) forming fibrils and with the neighboring chains (intermolecular) forming microbfibrils. The degree of polymerization within plant cellulose ranges from 4,000 to 10,000 [54, 55].

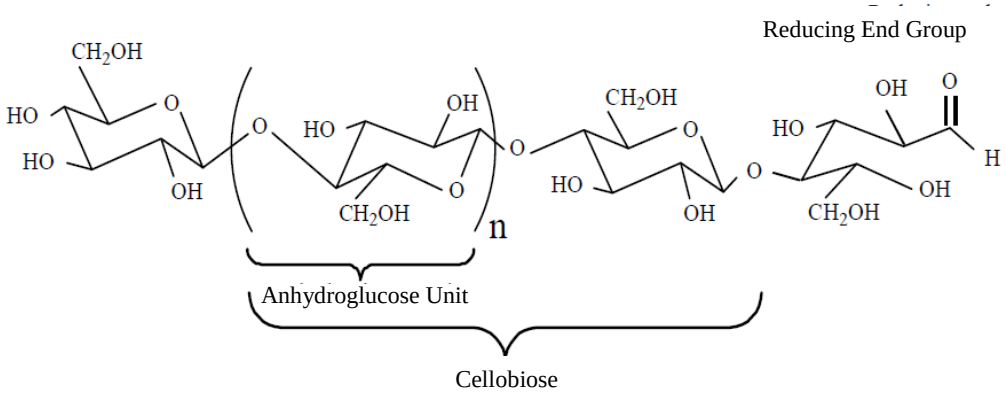

Figure 3. Basic chemical structure of plant cellulose showing the cellobiose repeat unit.

Hemicellulose

Hemicellulose is not a form of cellulose but a heterogeneous branched polysaccharide composed of several different sugar monomers: D-xylopyranose, D-glocopyranose, Dgalactopyranose, L-arabinofuranose, D-mannopyranose, and Dglucopyranosyluronic acid with small quantities of other sugars [56]. Unlike cellulose, the hemicellulose content varies between different plant sources. It is imbedded in the plant cell walls and act as an additional support structure linking the cellulose and lignin. These networks of cross-linked fibers permit the transfer of shear stresses between the cellulose microfibrils and the lignin [54]. The degree of polymerization for hemicellulose is typically around 200. Hemicellulose is mainly responsible for the water absorption in the fiber wall, biodegradation and thermal degradation due to greater solubility in solvents [45].

Lignin

Lignin is an amorphous, cross-linked polymer with a highly complex structure consisting of aliphatic and aromatic constituents. The lignin in plant fibers form a matrix sheath/adhesive around the microfibrils and fibers providing a compressive strength to the microfibrils preventing them from buckling under compressive loads [13]. Lignin is thermally stable; however, when exposed to ultraviolent (UV) light, lignin undergoes photochemical degradation.

Pectin

Pectins are composed of complex heteropolysaccharides of α-1, 4-linked galacturonic acid units, sugar units of various compositions (rhamnose, galactose and arabinose sugars, and their respective methyl esters [57]. Out of all compositions in plant fibers, pectin is the most hydrophilic compound due to the carboxylic acid groups. The hemicellulose, lignin and pectin collectively function as matrix and adhesive while aiding in holding the plant fiber cellulosic framework structure. Fiber separation is caused by the dissolution of both pectin and lignin using chemical aids.

Structural

Plant fiber cell walls are mainly made up of two distinct parts: the primary cell wall and secondary cell walls as shown in Figure 4. The fiber cell wall provides structural support, a porous medium for circulation and distribution of water, minerals and other nutrients, and a means to regulate the growth and protection from diseases. The middle lamella (ML) is the first layer formed during cell division and is composed of pectic

compounds and protein. The primary wall (P) forms after the middle lamella that consist of a rigid skeleton of microfibrils embedded in a gel-like matrix of mainly pectic compounds, hemicellulose and glycoprotein. The orientation of the microfibrils is often dispersed but shows varying degrees of alignment where cell elongation takes place [58].

The secondary wall is composed of highly oriented, crystalline microfibrils and amorphous lignin. The secondary wall can be further divided into three walls: S1, S2 and S3. Within the secondary walls, there are mesofibrils that are packed microfibrils that differ in composition and orientation (spiral angle). Spiral orientation of the microfibrils makes the fibers more ductile; parallel orientation to the fiber axis makes the fibers rigid [59]. S1 is the outer layer next to the primary wall with transversely oriented microfibrils that stabilize the fiber to lateral forces. S2 is the thickest layer in the secondary wall with axially oriented microfibrils that dominates tension properties [60]. S3 is the inner most wall with transversely oriented microfibrils and is more effective at stiffening the wall in the transverse plane, thus contributing to collapse resistance [58].

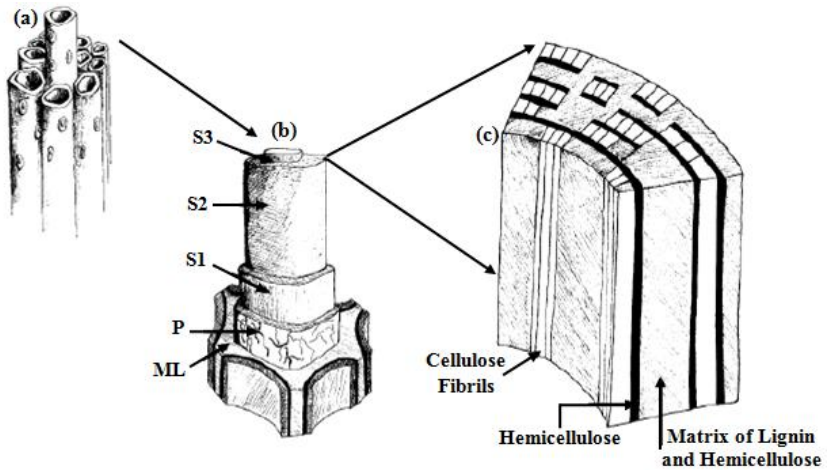

Figure 4. Cell wall of bast fibers containing (a) adjacent cells, (b) cell wall layers and (c) distribution of lignin, hemicellulose and cellulose in the secondary wall (adapted and modified from [61]).

Mechanical Properties

The spiral angle of the microfibrils and the percent of cellulose are the primary factors that determine the properties of natural fibers in addition to fiber length [54, 62]. Increasing cellulose content generally increases the tensile strength and Young's modulus while the microfibrillar angle determines the stiffness of the fibers [63]. Table 5 below shows fiber length, cellulose percentages and microfibrillar angle in comparison to some mechanical properties based from Table 3.

Table 5

Bast fiber mechanical properties based on fiber length, cellulose content and microfibrillar angle [45-49]

Fiber Type	Fiber Length (mm)	Cellulose Content (Wt. %)	Microfibrillar Angle (°)	Tensile Strength (GPa)	Young's Modulus (GPa)
Flax	10.0-40.0	71.0	5.00-10.0	0.35-1.04	60.0-80.0
Hemp	15.0-28.0	70.0-74.0	10.0	0.55-1.10	50.0-70.0
Jute	1.00-5.00	61.1-71.5	8.00	0.39-0.77	13.0-26.5
Kenaf	2.00-6.00	45.0-57.0	9.00-15.0	0.93	53.0
Ramie	60.0-260	68.6-76.2	7.50	0.40-0.94	44.0

Natural Fiber Advantages in the Automotive Industry

Automotive industries are focusing on developing products more eco-friendly and energy efficient on top of cost, weight-savings and end-of-life. As stated in the Introduction, natural fiber reinforced composites offer numerous advantages and

versatility with respect to the automotive industry. Natural fiber reinforced polymers are able to be 40 % lighter and 1/3 cheaper than glass reinforced polymers [12, 64]. In the processing aspect, 22-45 % of energy can be saved by utilizing natural fibers. Beckermann et al. reported that 65 wt. % hemp fiber reinforced PP composite can use 30,800 MJ/ton of processing energy while 30 wt. % glass reinforced PP composite can use 81,890 MJ/ton of processing energy [13]. Pervaiz et al. reported that 3 tons of CO_2 per ton of product produced could be saved using hemp fibers instead of glass fibers by converting the net energy consumed during composite production [65].

Acoustic absorption is an important property in designing interior automotive components. Natural fibers can improve material damping characteristics, which is an important factor in overall vehicle noise, vibration, and harshness performance (NVH). As a non-toxic, eco-friendly structural material, natural fibers have distinctive internal open cell structures that contribute to sound absorption coefficients [66].

Natural fibers will continue to have a positive growth on the global market due to its availability. Each year farmers harvest around 35 million tons of natural fibers and generate revenue over 36 million U.S. dollars according to the Food and Agricultural Organization [55]. The demand of natural fibers in the automotive applications to design and build lighter-weight, cost effective and environmentally friendly vehicles will continue to grow due to rising prices of petroleum-based products, strong government support to eco-friendly products, positive growth of end-use industries, efforts to reduce global warming and higher acceptance among consumers [67-69].

Natural Fiber Limiting Factors

Despite the advantages natural fibers possess over synthetic fibers, natural fibers have several disadvantages that affect the capabilites and properties used in the thermoplastic industry. Some of the main drawbacks that natural fibers have are poor binding/adhesion to hydrophobic polymer matrix materials, thermal instability and an affinity for moisture absorption [51, 70].

Interfacial Bonding

Natural fibers are derived from lignocelluloses that are strongly polarized with hydroxyl (OH) groups and hydrophilic in nature. Hemicellulose and pectin are the most hydrophilic components in plant fibers that contribute to the poor interfacial adhesion with thermoplastic matrices. Typical thermoplastic polymers are hydrophobic and are not attracted to the hydrophilic fibers which lowers the interfacial bonding, thus resulting in poor mechanical properties.

Thermal Stability

Natural fibers are inherently thermally unstable and start to degrade at temperatures around 200 °C. The processing temperature drawback results in limited manufacturing processes such as extrusion, injection molding and compression molding. According to Ghassemieh, fiber degradation occurs around 150 °C for long processing durations and 220 °C for short-term exposures [16]. When natural fibers are degraded, the fibers have poor interfacial adhesion, discoloration, and lower properties. Thus, natural fiber reinforced composites are limited to low temperature applications.

Moisture Absorption

One of the main disadvantages natural fibers possess is their high moisture uptake. Moisture absorption within natural fibers leads to fiber swelling and dimensional changes in the composite. As stated in the Interfacial Bonding section, natural fibers are very hydrophilic. Thus, additional moisture uptake reduces the adhesion between fiber and matrix. Joseph et al. reported the debonding between fiber and matrix may be caused by the osmotic pressure pockets at the surface of the fiber, leading to leaching of water-soluble substances from the fiber surfaces [71]. According to Holbery et al., temperature, relative humidity, and air velocity are the three factors that can determine the rate at which moisture is removed from lignocellulosic materials [72].

Kinetics of Moisture Absorption. Moisture absorption into fiber reinforced composites can occur by three different mechanisms [73]. The most common method consists of the diffusion of water molecules inside the microholes between polymer chains. The second mechanism is through the capillary transport of water molecules into the gaps and flaws at the interface between fiber and polymer. This phenomenon is due to the incomplete wettability and impregnation. The last mechanism occurs by the transportation of water molecules by the micro cracks in the matrix formed during the compounding process.

These three diffusion mechanisms can be modeled theoretically by the shape of the absorption curve by the empirical equation:

$$\frac{M_t}{M_m} = kt^n \tag{2}$$

where M_t is the moisture content at time t, M_m is the moisture content at the equilibrium and k and n are diffusion kinetic constants. The constant k provides an idea about the interaction of moisture within the composite material. The coefficient n has three different behaviors of diffusion; for Fickian diffusion, $n = 0.5$, non-Fickian, $n=1$, and anomalous when $0.5 < n < 1$ [73].

Several researchers state that moisture uptake in natural fiber reinforced composites usually follow the Fickian diffusion behavior [74]. Fickian diffusion follows Fick's law, which states that the absorbed mass of water increases linearly with the square root of time, and then gradually slows until an equilibrium plateau is reached. The diffusion coefficient or diffusivity, D, characterizes the ability of water molecules to penetrate through the composite and can be calculated by a one-dimensional approach from the following equation:

$$D = \pi\left(\frac{h\theta}{4Q_\infty}\right)^2 \tag{3}$$

where θ is the slope of the linear portion of the absorption curve, h is the initial sample thickness and Q is the mass of absorbed water at infinite time.

Chemical Treatments and Agents

To fully utilize the mechanical properties of the reinforcing fibers to improve the composite properties, the adhesion between the fiber and matrix need improvement. To obtain better interfacial bonding between the fiber and matrix, improve thermal stability, reduce the moisture uptake in fibers and impart dimensional stability and

thermoplasticity, fibers are chemically treated to remove the non-cellulosic components and/or the matrix is modified with the addition of coupling agents. Both the chemical treatment and coupling agent are further discussed below.

Alkaline Treatment

Alkaline treatments or mercerization are the most commonly used chemical treatment of natural fibers to reinforce thermoplastics [75]. Ionization of the hydroxyl group to the alkoxides is due to adding aqueous sodium hydroxide (NaOH). Alkaline chemical treatment increases the surface roughness by distributing the hydrogen bonding in the network structure to provide additional sites for mechanical locking. It selectively degrades a certain amount of lignin and pectin and facilitates the exposure of reactive OH groups on the fiber surface. This removal increases the bonding between the fiber and the polymer matrix. In addition to the extraction of lignin and hemicellulose compounds, the alkaline treatment increases the number of reaction sites by increasing the amount of cellulose exposed on the fiber surface [76, 77].

Alkaline processing directly influences the cellulosic fibril, degree of polymerization and extraction of lignin and hemicellulosic compounds. Li et al. studied sisal fibers at different NaOH concentrations, temperature, time and pressure [50]. Sisal fibers treated with 5 % aqueous NaOH for 72 hours at room temperature and another set with 2 % NaOH for 90 seconds at 200 °C at 1.5 MPa pressure both had a positive effect on the fiber surface by increasing the amorphous cellulose content at the expense of crystalline cellulose [50, 78]. Ray et al. studied 5 % NaOH treated jute fibers at various hours of treatment [79]. After 4, 6 and 8 hours of treatment, the treated jute fibers

increased their modulus by 12 %, 68 % and 79 %, respectively. Kalia et al. reported that flax fibers soaked in 5, 10 or 18 % NaOH were the best concentration to increase the possible number of reactive sites, therefore allowing better fiber wetting [76].

Maleated Coupling Agents

Maleated coupling agents are used to modify the fiber and to strengthen fiber reinforcements. This coupling agent acts as a compatibilizer achieving better interfacial bonding and mechanical properties of the composite. The PP chain interacts with the maleic anhydride (MA) to be cohesive and form maleic anhydride grafted polypropylene (MAPP). Through polymer entanglements, MAPP coupling agent serves as a 'bridge' between the polar natural fibers and the nonpolar PP matrix. The fiber surface interacts strongly with the MA functional group through covalent and hydrogen bonding and the OH groups on the surface of the cellulose and lignin. By chain entanglements, the unreactive PP matrix is then combined with MAPP. The chain entanglements are an important factor in determining the mechanical properties up to and above the glass transition temperature of the matrix [13]. The chains can entangle if the MAPP polymer chains are long enough; however, the viscosity of the coupling agent increases and results in poor fiber wetting. The wettability of the fiber can be increased by increasing the surface energy of cellulose fiber to a level close to the surface energy of the matrix [50]. Overall, this coupling agent can reduce the water absorption and increase the modulus, hardness, and impact strength of the natural fiber-reinforced composites [13, 80].

Sanadi et al. investigated 3 wt. % MAPP with 50 wt. % kenaf fiber reinforced composites [80]. The tensile strength and Young's modulus increased 88 % and 350 %,

respectively. Mfala reported that 6 hours of 20 % maleic acid treatment on flax fiber reinforced PP composites increased the flexural strength by 150 % from that of neat PP [82].

Industrial Hemp Fibers

Out of all the bast fibers, hemp fibers have been increasingly used in the automotive industry because of their mechanical properties and cost. Hemp fiber is among the strongest and stiffest natural fiber available and can reach a tensile strength of 1,100 MPa and Young's modulus of 70 GPa. Hemp fibers are used mostly as automotive interior components and now expanding to exterior components due to its mechanical properties, biodegradability and lightweight design [83].

Background

Industrial hemp fiber (*Cannabis Sativa* L.) has been cultivated for over 6,000 years and is one of the oldest non-food crops. Hemp originated from Central Asia and was an important fiber cultivated from the 16^{th} to the 18^{th} century that branched out from the Equator to the polar circle [84]. Then in the 19^{th} and 20^{th} centuries, there was a decline in hemp cultivation due to the large scale production of cotton, introduction of synthetic fibers and legislation related to the control of psychoactive substances such as marijuana [85].

Hemp fibers can grow in moderately cool climates in soils that are high in organic matter with a neutral or slightly alkaline pH level. Water is crucial between the first 30-40 growth days. Hemp is a hardy plant that grows extremely fast, exceeding a growth rate

of one inch per day [13]. Bennett et al. reported for maximum hemp fiber production, the fibers should be planted in a tight formation [86]. Hemp is an annual plant that has five lifecycle stages: germination, growth, flowering, seed formation and death. The chemical composition and fiber properties change as the fibers grow, making harvest timing important to achieve quality fibers. Hemp fibers are harvested when 50 % of the seeds resist compression; but if harvested earlier, the fibers are weaker and less dense [13].

Industrial hemp fiber and marijuana are completely different varieties of the same plant species and are sometimes confused for one another. DeMeijer et al. concluded in a study of 97 Cannabis strains that there was no way to distinguish between marijuana and hemp varieties without a chemical analysis of the psychoactive ingredient delta-9-tertahydrocannabinol (THC) [87]. Industrial hemp fiber contains less than 1 % THC while marijuana contains 3-15 % THC.

Europe, today, produces up to 25 tons of dry matter per hectare per year of hemp fibers and is considered one of the faster growing biomasses known [88]. Countries such as Great Britain, Germany, Austria, Switzerland, Canada, Australia, China, Russia and Hungary have already legalized hemp production. With Canada allowing production, the U.S. has raised questions about the potential commercial market demand for industrial hemp products since hemp cannot be commercially grown in the U.S. [89]. Several states have been trying to allow industrial hemp cultivation. Imports of raw hemp fibers, including hemp seeds and fibers, into the U.S. were nearly $10.5 million in 2010 [90].

Hemp Fiber Reinforced PP Composites

Typically hemp fiber and PP in a non-woven mat form are compression molded to produce automotive parts [91]. This research will focus on analyzing an alternative form of hemp (long fibers) and processing method (compounding-extrusion-compression molding) to optimize hemp fiber reinforced PP composites.

As stated in the Matrix section, PP is one of the most common thermoplastics utilized in natural fiber composites. Besides being cost effective, recyclable and lightweight, PP has a low level of moisture absorption that will reduce the moisture uptake of hemp fiber reinforced PP composites [13]. Even though PP is one of the weaker thermoplastics compared to PVC and low and high density PE, PP generally has a higher tensile strength. Thus, PP is a suitable thermoplastic matrix for hemp fibers in the automotive applications.

Hemp fiber reinforced PP composites are increasingly being utilized in several automotive and transportation applications. For example, Chrysler was the first automaker to use EcoCor, a bio-based composite developed by Johnson Controls, that has a combination of 25 % hemp and 25 % kenaf fiber reinforced PP composites in the interior door panels of the Sebring [92]. Hill et al. reported that hemp fiber reinforced PP composites had a 26 % weight reduction compared to glass fiber reinforced composites in the auto insulation panel component [93]. Ford is conducting trials on injection molded hemp fiber reinforced PP composites in engine shields [94].

EXPERIMENTAL

Introduction

The purpose of this research is to maintain critical fiber length while optimizing the mechanical and environmental properties of hemp reinforced PP composites. In order to achieve this objective, the fiber length and diameter were analyzed at each processing step with various processing parameters before evaluating the mechanical and environmental properties. A Design of Experiment (DOE) approach was utilized to obtain meaningful and statistically sound conclusions.

Based on literature, chemical treatments and chemical agents were evaluated to minimize the time and cost of fiber and matrix modifications while obtaining better properties. Composites were produced by compounding chopped hemp fibers and PP pellets in a twin screw extruder, chopping the extruded LFTs, extruding the chopped LFTs through a single screw extruder and compression molding the composites into test plates.

The hemp fiber reinforced PP composites were analyzed to evaluate properties such as strength, modulus, impact performance, interfacial adhesion, moisture absorption and ultraviolent (UV) radiation resistance to obtain the overall best variance to be manufactured for the prototype component.

Materials

Industrial hemp fibers were supplied by Composites Innovation Centre (CIC), Canada, as the composite reinforcement. Due to variations in hemp crop production and natural retting processes, several hundred pounds of hemp fibers were supplied to reduce variability caused from using different stock/batches. PP pellets were procured from the DOW Chemical Company as the matrix material. The fiber and matrix treatments were supplied from various companies, NaOH pellets from Fisher Scientific and Polybond 3200 (MAPP), having 1.0 wt. % maleic anhydride, from Chemtura.

Fiber Length and Aspect Ratio Evaluation

Several fiber length studies have been made on the single screw extruder at UAB but minimal research has been done on the twin screw extruder. Herrera-Estrada and Mfala reported that the twin screw extruder caused severe fiber attrition but better wetting of the fibers than using the single screw extruder [82, 95]. To analyze the fiber attrition on the twin screw extruder, a DOE approach was used, using the software JMP® 9 to aid in structurally organizing the design process to obtain the minimum number of trials to run, determine the overall best trial and to reduce the influence of the experimental error. Response(s) and factors were inputted into the software to compute a certain number of trials based off the Yate's order. Once the best parameters were defined for minimal fiber attrition in the twin screw extruding process, the overall processing for fiber length and diameter were analyzed.

A typical burn-off test to analyze fiber length would not work for hemp fiber with PP due to the thermal stability properties of the hemp fibers. To elevate the temperature

to burn off the resin, the hemp fibers would disintegrate. Thus, the PP was replaced with a water-soluble polymer polyvinyl alcohol (PVA) that had a similar viscosity flow as PP. The PVA could be washed out leaving the hemp fibers to be analyzed.

DOE Response and Factors

The DOE response being analyzed was the hemp fiber length (mm). To ensure maximum desirability, an average unprocessed fiber length of 25.4 mm was inputted in the software. The unprocessed fiber length of 25.4 mm was used based on commercially available LFT material. There are, however, several factors that affect the hemp fiber length when compounding. The factors can be further subdivided into studied factors and fixed/constant factors as shown in Table 6 that were based on prior experimentation. The zone temperatures in the Leistritz MICRO 18 twin screw extruder were grouped based on the compounding, feeding and shearing areas illustrated in Figure 5.

Table 6

Studied factors vs. fixed/constant factors for DOE analysis

Studied Factors	Fixed/Constant Factors
Zone B Temperature	Hemp Form
Zone C Temperature	Hemp and PVA Feed Rate
Screw Speed	Side Stuffer Screw Speed
Weight Percentage of NaOH	Zone A Temperature
	Coolant System

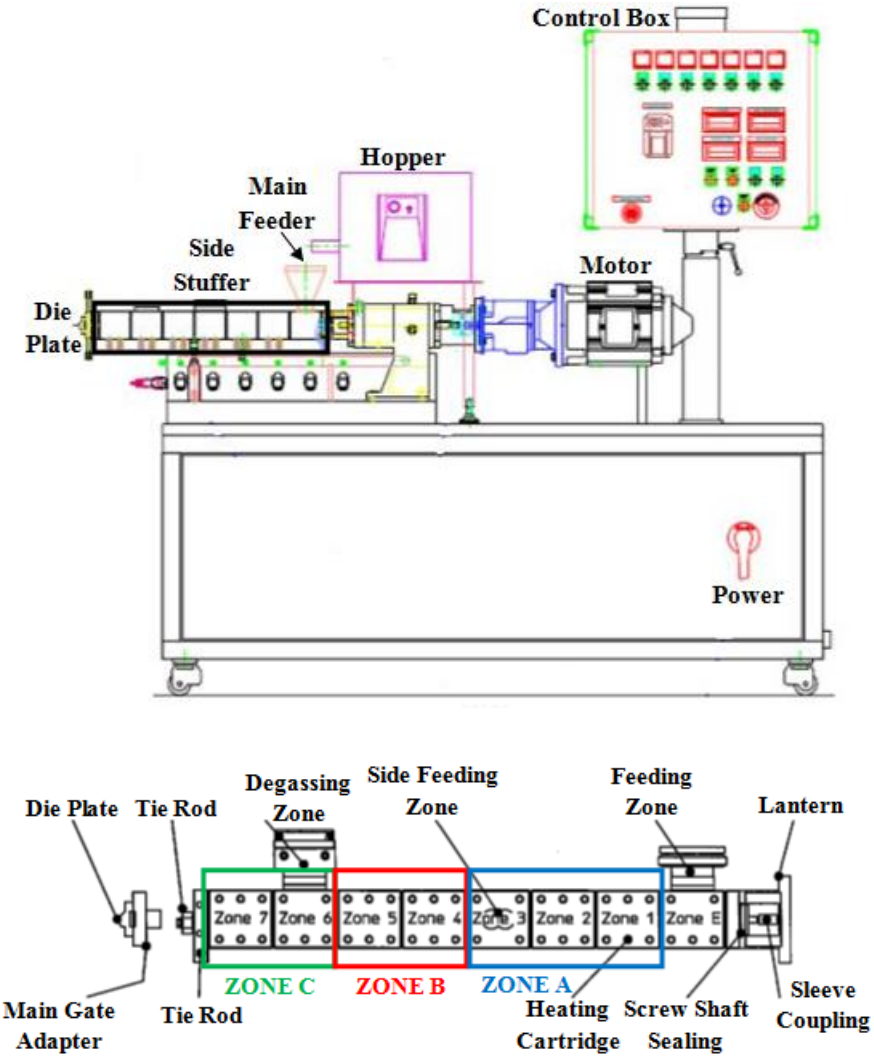

Figure 5. Schematic setup of the Leistritz MICRO 18 twin screw extruder with detailed view of the temperature zones (schematic from Leistritz manual).

The four studied factors were inputted to construct the DOE: zone B temperature, zone C temperature, screw speed and fiber treatment. Distinguishing and reducing which factors are of importance will greatly decrease the experimental error within the software. The temperature range and chemical fiber treatment were based on the literature. The screw speed range was decided based on prior research of the ability to process all the

needed amount of fibers separately from the resin to obtain a 15 wt. % fiber amount. Table 7 shows the four factors' minimum and maximum range inputted into the software. A 2^4 factorial design was used based off the number of factors following the classic trial order, Yates order.

Table 7

Factors and study domains

Factors	Low Level (-)	High Level (+)
Zone B Temperature (°C)	185	220
Zone C Temperature (°C)	185	220
Screw Speed (rpm)	80	120
Fiber Treatment-NaOH (wt. %)	0	5

Fiber Preparation for Preliminary Trials

Hemp fibers were dried before any treatment was done at 50 °C for 48 hours. The hemp fibers were divided into 50 g each of an untreated and treated batch. The treated batch was soaked in 5 wt. % NaOH solution at ambient temperature. The fibers were kept immersed for an hour and were then thoroughly washed with water to remove any traces of alkali on the fiber surface. In addition, the untreated batch was washed with water. Both the untreated and treated fibers were separately dried at 50 °C for 48 hours.

Preliminary Twin Screw Processing

Before processing 15 wt. % hemp fiber reinforced PVA composites, the hemp fiber batches were pulled and separated thoroughly to get rid of the clumped fibers. The zone temperatures and screw speed were set accordingly to each trial. Zones 1-3 temperatures were set to 180 °C. The side stuffer screw speed, hemp fiber feed rate and PVA feed rate were set at a constant rate of 40 rpm, 24.0 g/min and 4.24 g/min, respectively. The PVA was fed through the main feeder opening while the fibers were fed through the side stuffer manually. A tape segment of approximately 20.0 g was pulled off and set to cool. This process was repeated for each of the trials.

Twin Screw and Plasticator Processing

Two sets of hemp fiber batches were analyzed for this research, 15 wt. % and 30 wt. % hemp fiber reinforced PVA. Before processing, 10.0 g of each fiber batch was set aside for fiber length and diameter analysis. Similar to the Preliminary Compound Processing, untreated hemp fibers were pulled and separated thoroughly to remove the clumped fibers and compounded with PVA in the twin screw extruder. Zones 1-3 temperature were set to 180 °C and Zones 4-7 temperature did not exceed 185 °C. Table 8 below shows the twin screw parameter for each of the two batches. A tape segment approximately 20.0 g was pulled off and set to cool for analysis. The extruded tape LFT was air cooled and chopped to approximately 38.1 mm. Roughly 10.0 g of the chopped LFT was set aside for analysis. The chopped LFTs were then fed through a low shear single screw plasticator. The temperature in the plasticator did not exceed 190 °C. A 30.0 g extruded charge was set aside for the last analysis set.

Table 8

Twin screw parameters for 15 wt. % and 30 wt. % hemp fiber batch

Hemp Fiber Content (wt. %)	Fiber Feed Rate (g/min)	Resin Feed Rate (g/min)	Screw Speed (rpm)	Side Stuffer Screw Speed (rpm)
15	24.0	4.24	80	40
30	20.0	8.57	90	60

Fiber Extraction

Each material segment was heated up at 250 °C in water to dissolve the PVA. Every hour the fibers were strained and replaced into the beaker with clean water. This process was repeated until the PVA was completely removed from the fibers. Each set of fibers were then strained and dried separately at 50 °C for 48 hours.

Fiber Length and Diameter Analysis

For each processing and trial sets, macrophotographs were taken for the fiber lengths, while the fiber diameter pictures were taken with a Stemi SV II stereoscope. Each picture was saved as a TIF file and was opened in an image processing, enhancement and analysis software called Image-Pro® Plus 7.0. This software calibrated each image and measured the fiber length and diameter.

Hemp Fiber Reinforced Polypropylene Composite Processing

Experimental Setup

Table 9 below shows the nomenclature used for all the variances for both the 15 wt. % and 30 wt. % hemp fiber reinforced PP trials. The variances in the 15 wt. % trials were based on the literature, and the 30 wt. % was based off the 15 wt. % preliminary data results.

Table 9

Nomenclature used for 15 wt. % and 30 wt. % trial variances

Abbreviation	15 wt. % Trial	Abbreviation	30 wt. % Trial
PP	Neat PP	30-A	Untreated Hemp Fiber
PP-MAPP	Neat PP + 5 wt. % Polybond	30-B	5 wt. % NaOH
15-A	Untreated Hemp Fiber	30-C	5 wt. % MAPP
15-B	5 wt. % NaOH	30-D	5 wt. % NaOH + 5 wt. % MAPP
15-B2	10 wt. % NaOH		
15-C	5 wt. % MAPP		
15-D	5 wt. % NaOH + 5 wt. % MAPP		

Fiber Treatment and Coupling Agent Processing

Fiber treatment was similar to the Fiber Preparation for Preliminary Trials section. Hemp fibers were dried at 50 °C for 48 hours before any treatment or processing was done. Pre-dried fibers were soaked in 5 wt. % NaOH and 10 wt. % NaOH solution at ambient temperature. The fibers were kept immersed for an hour and then thoroughly washed with water to remove any traces of alkali on the fiber surface. The treated fibers were then dried at 50 °C for 48 hours.

5 wt. % Polybond 3200 was added to the pre-weighed PP batch with respect to the 15 wt. % and 30 wt. % hemp fiber. The MAPP mixture was then blended with the PP before processing.

Manufacturing and Processing

Figure 6 below illustrates the overall manufacturing process of hemp fiber reinforced PP composites. The processing method is exactly the same as in the Compound-Extrusion Processing section, excluding the segments taken out for fiber length and diameter analysis. After the charge was extruded in the low shear plasticator, the extruded charge was then compression molded into a test plate at 17 MPa and held for 2 minutes. The tool temperature was set at 77 °C.

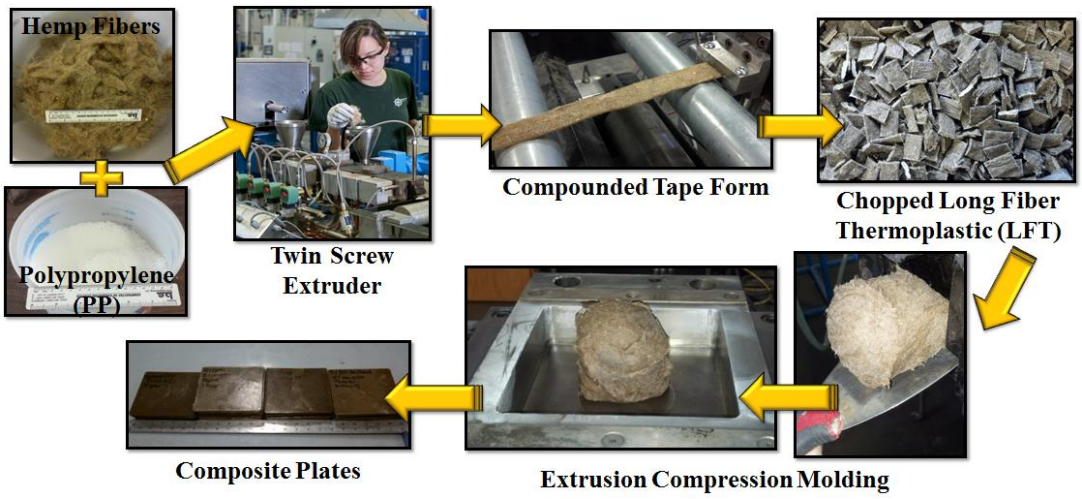

Figure 6. Compounding-extrusion-compression molding process of hemp fiber reinforced PP composites.

Testing Methods and Characterization

Mechanical Testing

Flexural Testing

Flexural testing was conducted according to ASTM D 790-03 Standard Test Methods for Flexural Properties of Unreinforced and Reinforced Plastics and Electrical Insulating Materials using an INSTRON SATEC APEX T 5000 screw driven machine with a crosshead speed of 5 mm/min. The dimensions of each sample were based on the sample thickness. Five samples of each of the trial sets were tested, and the average flexural strength and modulus were calculated.

Tensile Testing

Tensile testing was conducted according to ASTM D 638-03 Standard Test Method for Tensile Properties of Plastics using the MTS 810 Material Test System with a MTS Extensometer to measure the strain. All tensile sample dimensions were 19.0 mm by 152 mm. Five samples of each of the trial sets were tested, and the average tensile strength and modulus were calculated

Impact Testing

Impact testing was performed using the Tinius Olsen Model Impact 104 according to the ASTM D 256-10 Standard Test Methods for Determining the Izod Pendulum Impact Resistance of Plastics. All samples were cut into 63.5 mm by 12.7 mm rectangular specimens with a 45 °, 2.10 mm deep notch. Ten samples from each trial sets

were tested. The testing fixture automatically calculates the impact resistance (J/m) and impact strength (kJ/m^2) based on the specimen dimensions and impact energy (J).

Environmental Testing

Hygrothermal and UV exposure testing were conducted only on the 30 wt. % hemp fiber reinforced PP variances.

Hygrothermal Testing

Moisture absorption testing was conducted according to ASTM D 570-98 Standard Test Method for Water Absorption of Plastics. Two sets of hygrothermal aging tests were conducted for this research. The first hygrothermal test was an accelerated water absorption study. The samples were fully submerged in a control fixture maintaining a temperature of 40 °C. A total of 10 flexural, 10 tensile and 20 impact samples were tested for moisture uptake for each variance set, half of each set was tested as wet samples after saturation and the other half was tested as re-dried samples after saturation.

The second hygrothermal test determined how much moisture was absorbed in a realistic environment. Based off the weather and humidity in the United States and western Canada, the average high temperature and humidity were approximately 40 °C and 65 % humidity. Samples were sent to CIC for the realistic hygrothermal testing using the Thermotron SM-4-8200 environmental chamber. Due to the time restraints, only 2 samples of each testing set from each variance were weighed for water absorption for approximately a month and a half.

For both hygrothermal tests, the samples were taken out periodically (based on the square root of time in hours) and weighed immediately after wiping the water residue off the sample surface using a precise four digit balance. The moisture absorption percentage, *M*, can be calculated by the following equation:

$$M\ (\%) = \frac{W_t - W_0}{W_0} \tag{4}$$

where W_t is the weight of the sample at time *t* and W_0 is the initial weight of the dried sample at time=0. This procedure was repeated for the accelerated hygrothermal test until each of the variances reached full saturation. Samples from both sets were tested afterwards for flexural and tensile strength and modulus and impact strength comparing the before aging (control) samples to both wet samples after saturation and re-dried samples after saturation. Table 10 below shows the nomenclature used for both the hygrothermal set samples.

Table 10. *Nomenclature used for hygrothermal samples*

Natural Fiber Wt. %	Hygrothermal Set	Variance	Condition
30	(X) Accelerated	(A) Untreated	(O) Control
	(R) Realistic	(B) 5 wt. % NaOH	(W) Wet
		(C) 5 wt. % MAPP	(RD) Re-dried
		(D) 5 wt. % NaOH + 5 wt. % MAPP	

UV Exposure Testing

UV exposure testing was carried out according to ASTM D 4329-99 Standard Practice for Fluorescent UV Exposure of Plastics. Due to the dimensions of the UV RPR 200 reactor chamber, three flexural samples of each set and exposure time were tested and recorded for discoloration and deterioration. Flexural samples were exposed for 500 and 1,000 hours. Flexural testing was conducted afterwards comparing the control samples to the UV exposed samples.

Microscopy Analysis

Fiber surface topography and composite fracture surface morphology were studied using a FEI QUANTA FEG 650 scanning electron microscope (SEM). All samples were mounted with carbon tape and then sputter-coated with palladium/gold to provide enhanced conductivity prior to SEM observation. The SEM was operated either at 20 kV or 30 kV for all specimens.

Female-Male Tool Die Machining

MacDon Industries in Manitoba, Canada, provided a model drawing of the duct-screen cleaner component that was redesigned to be compatible with the compression molding process as shown in Figure 7. The modeling file was imported to HyperMesh to remove any undercuts and unwanted features and to separate the outer and inner layer of the component. These layers acted as the male and female portion of the tool die. The outer and inner layers of the component were then exported to PTC Creo Parametric to

complete the male and female tool die. 1 % shrinkage was taken into account for the design. The models were then machined using a Haas CNC mill using A36 steel.

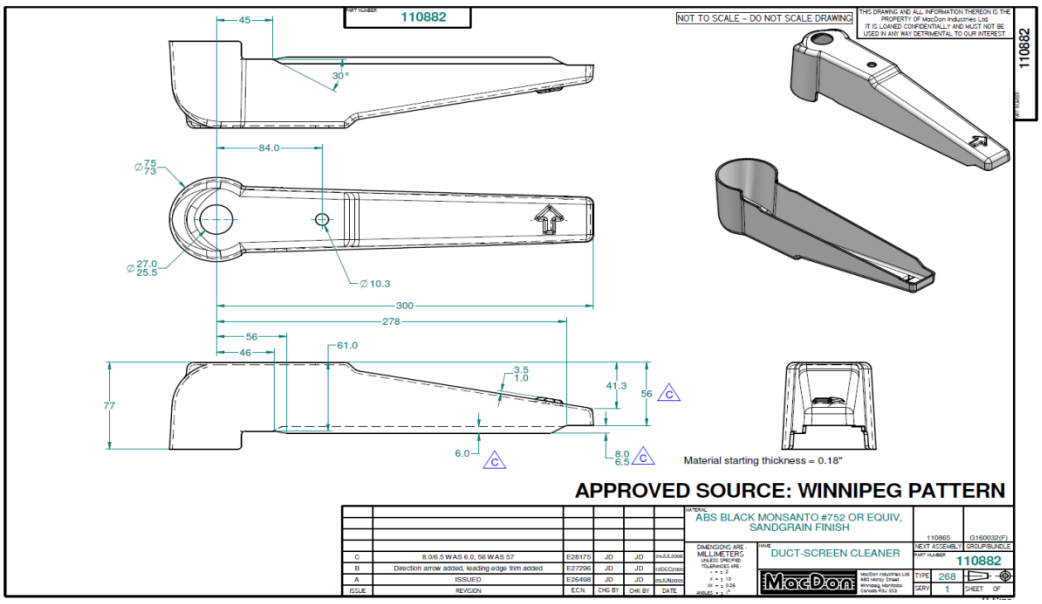

Figure 7. Duct-screen cleaner drawing provided by MacDon Industries.

RESULTS AND DISCUSSION

Fiber Aspect Ratio Evaluation

DOE Preliminary Results

Sixteen trials were computed after the response and factors were inputted. Table 11 below shows the average fiber lengths for the twin screw extruder process. Each trail obtained a coefficient of variation (CV) value at or less than 0.05 to obtain at least a 95 % confidence interval (CI). Trails 8, 12, 15 and 16 were very difficult to measure due to their extremely small length and were set with a random value of 2.00 mm.

Table 11

Designed experiment for studying hemp fiber length on the twin screw extruder

Trial	Zone B Temperature (°C)	Zone C Temperature (°C)	Screw Speed (rpm)	Fiber Treatment (wt. %)	Fiber Length (mm)
1	185	185	80	0	11.6
2	220	185	80	0	10.0
3	185	220	80	0	14.5
4	220	220	80	0	2.00
5	185	185	120	0	17.1
6	220	185	120	0	12.0
7	185	220	120	0	12.0
8	220	220	120	0	2.00
9	185	185	80	5	15.4
10	220	185	80	5	17.0
11	185	220	80	5	14.5
12	220	220	80	5	2.00
13	185	185	120	5	14.9
14	220	185	120	5	15.7
15	185	220	120	5	2.00
16	220	220	120	5	2.00

Desirability Function

The Desirability Function in the Prediction Profiler can find the best compromise among the several trials. Setting the Prediction Profiler to Maximize Desirabily, the maximum fiber length of 17.1 mm was computed with the following factor values: zone B temperature at 185 °C, zone C temperature at 185 °C, screw speed at 120 rpm and 0 wt. % chemical treatment as shown in Figure 8. Overall, there was a 30 % decrease from the original unprocessed fiber length of 25.4 mm.

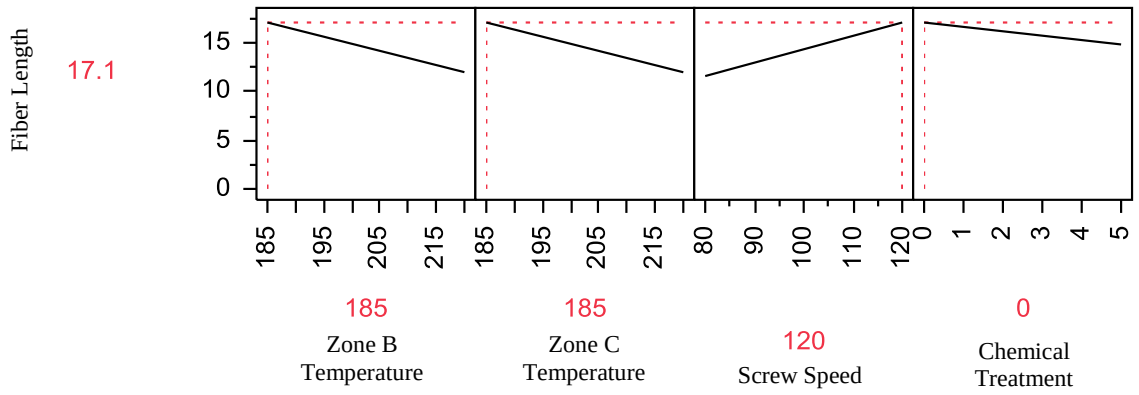

Figure 8. DOE Maximum Desirability for hemp fiber length.

Overall Fiber Aspect Ratio Analysis

Since the fiber length was optimized during the twin screw compounding process, the overall process fiber aspect ratio was then analzyed. Figures 9 and 10 below show the distribution of fiber lengths before and after compounding and before and after the extrusion process. Fiber lengths after the compounding process were mainly between the 20-30 mm; after the plasticator process, fiber lengths were mainly between 10-20 mm. The compounding process had a wide range of fiber length, whereas the palsticator processing narrowed the distribution of fiber lengths.

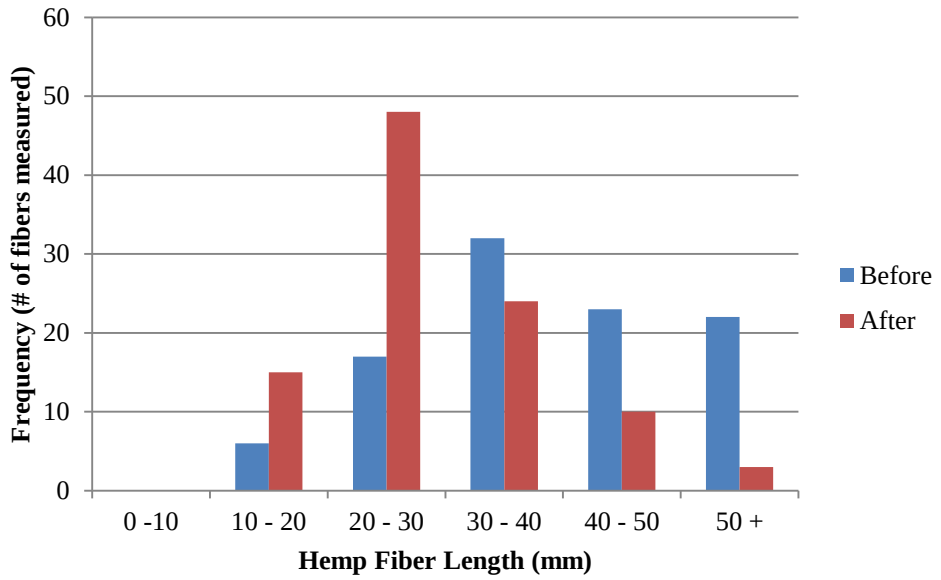

Figure 9. Hemp fiber length before and after twin screw compounding process.

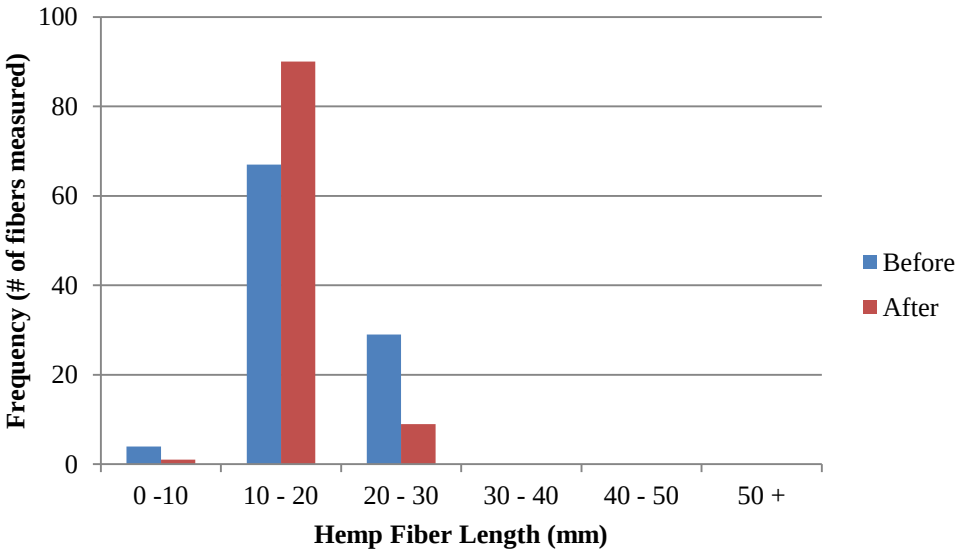

Figure 10. Hemp fiber length before and after extrusion process.

Table 12 below shows the average fiber length and diameter of each processing stage with the ending aspect ratio. Hemp fiber length retained over 60 % of its original

length, based on 25.4 mm fiber length, with an aspect ratio of 628. When processing with a higher fiber load in an extrusion process, higher shear stresses occur due to the fibers higher viscosity and fibril-fiber interaction resulting in lower aspect ratio [96].

Table 12

Aspect ratio of hemp fiber overall processing analysis

Composite Process		Average Length (mm)	Average Diameter (mm)
Twin Screw	Before	36.4	0.04
	After	29.1	0.03
Plasticator	Before (Chopped)	17.4	0.03
	After	15.7	0.03
ASPECT RATIO		628	

The fiber length retention was optimized from several outside factors in addition to the ones previously mentioned in Table 6. The screws within the twin screw extruder were selected based off of minimal shearing regions. The screws chosen have various kneading areas with twisting angles of 30°, 60° and/or 90° that are located in Zones 4-7 that results in less shearing to reduce fiber attrition.

In addition to the screw configuration, a side stuffer was introduced into Zone 4. A crammer was originally on the twin screw but did not allow natural fibers to feed properly into the extruder. The natural fibers were too light to allow the crammer design to push the fibers into the extruder. From previous research done from Herrera-Estrada and Mfala, the fibers were introduced into the main feeder where the fibers went through

the whole barrel length and had severe fiber length degradation [82, 95]. Thus, a side stuffer with its own twin screws allowed the fibers to enter the extruder into less regions of the barrel resulting in minimal shearing.

The final factor that aided in minimal fiber length attrition was the design of a new die plate. Typical geometry of LFTs are the spaghetti, string-like shapes that are chopped into pellets. This die configuration causes high shear, fiber break-ups and the material flow to become difficult. The back pressure of the twin screw extruder will spike to a high pressure and stop the screws from co-rotating. Therefore, a die plate with a ribbon, tape form geometry with smooth, extended transitions was designed to allow the composite to flow without any barriers and resistance while maintaing the fiber aspect ratio.

Hemp Fiber Reinforced PP Composites

Hemp Fiber Surface Morphology

Figure 11 shows the surfaces of the untreated, 5 wt. % NaOH and 10 wt. % NaOH treated hemp fibers. The untreated fibers in Figure 11a have uneven deposits impurities on its surface. In contrast, the alkali treatment of the fibers led to a cleaner, yet rougher surface than seen in the untreated fiber surface as shown in Figures 11b and c. The increase in NaOH concentration removed most surface impurities resulting in the rougher, cleaner surface. The alkali treatment is expected to increase the surface roughness by distributing the hydrogen bonding in the network structure to provide additional sites for mechanical interlocking [13]. Thus, the bonding/adhesion between the fiber and matrix at the interface should improve.

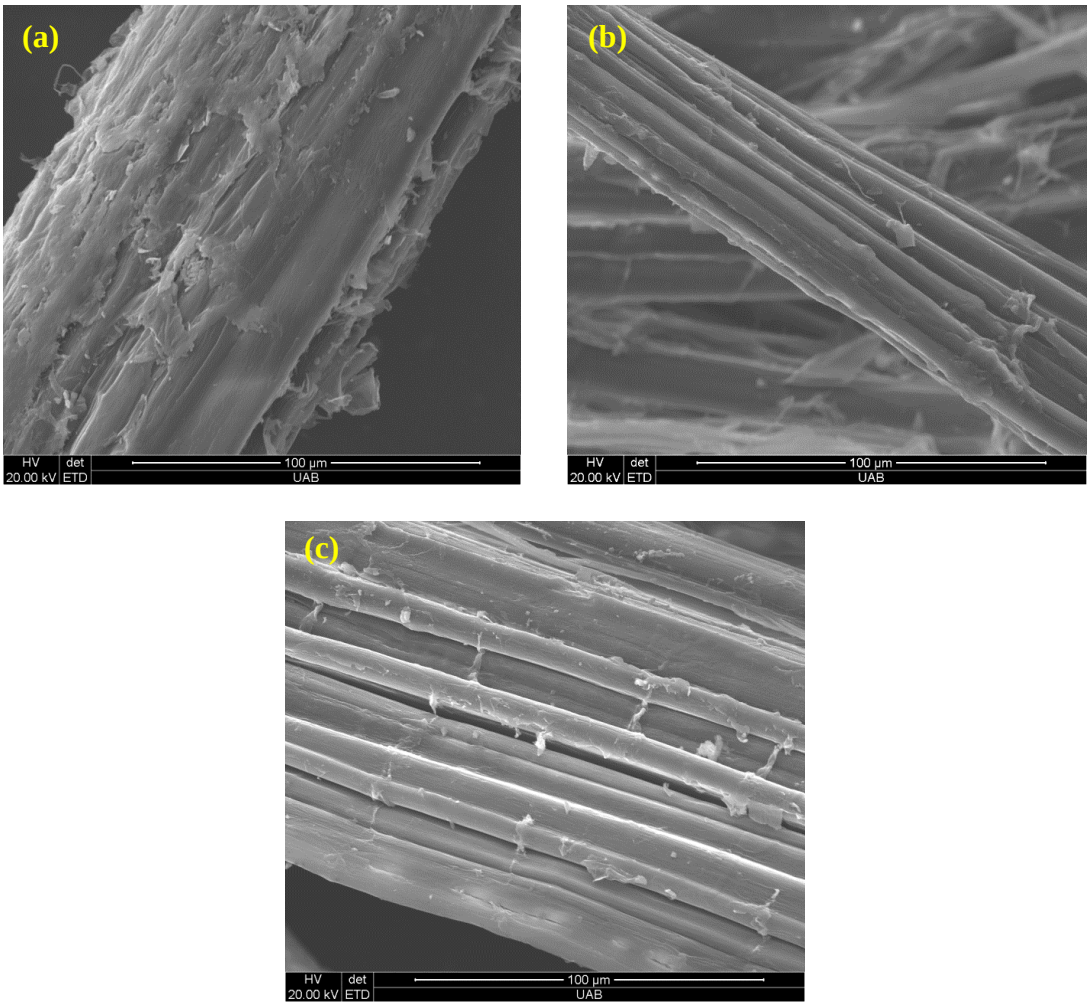

Figure 11. SEM images of hemp fiber surfaces of (a) untreated, (b) 5 wt. % NaOH and (c) 10 wt. % NaOH.

Preliminary Data: 15 wt. % Hemp Reinforced PP Composites

Figures 12-15 compare the flexural and tensile strength and modulus of each variance. The increase in NaOH concentration increased the mechanical properties due to the removal of unwanted impurities that led to cleaner and rougher fiber surfaces. However, the addition of the MAPP coupling agent showed better results than the NaOH treated hemp fibers. 15-C addition had the highest flexural strength of 35.4 MPa, flexural

modulus of 1.12 GPa, tensile strength of 24.2 MPa and modulus of elasticity of 2.23 GPa. The surface of the fiber with MAPP addition allowed direct bonding between the MA functional group and microfibrils cellulose OH groups [50]. This interaction allowed the flexural and tensile strength and modulus properties to increase, compared to PP, respectively, by 37 %, 37 %, 68 % and 213 %. 15-D had slightly better flexural properties than 15-C; however, the tensile properties had roughly the same values of the 15-B.

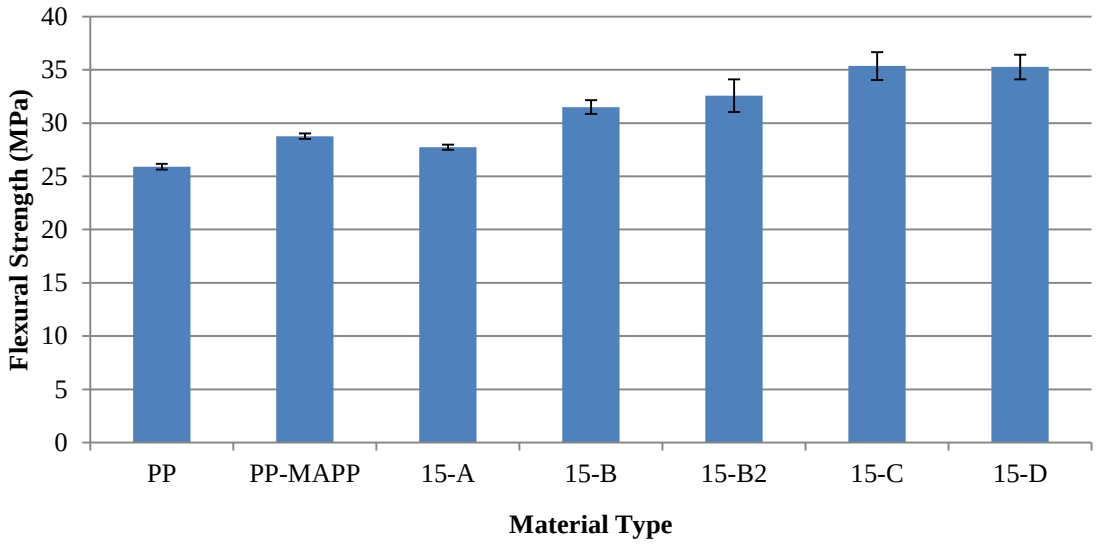

Figure 12. Flexural strength of 15 wt. % hemp fiber reinforced PP composite variances. (A-untreated, B-5 wt. % NaOH, B2-10 wt. % NaOH, C-5 wt. % MAPP and D-5 wt. % NaOH + 5 wt. % MAPP)

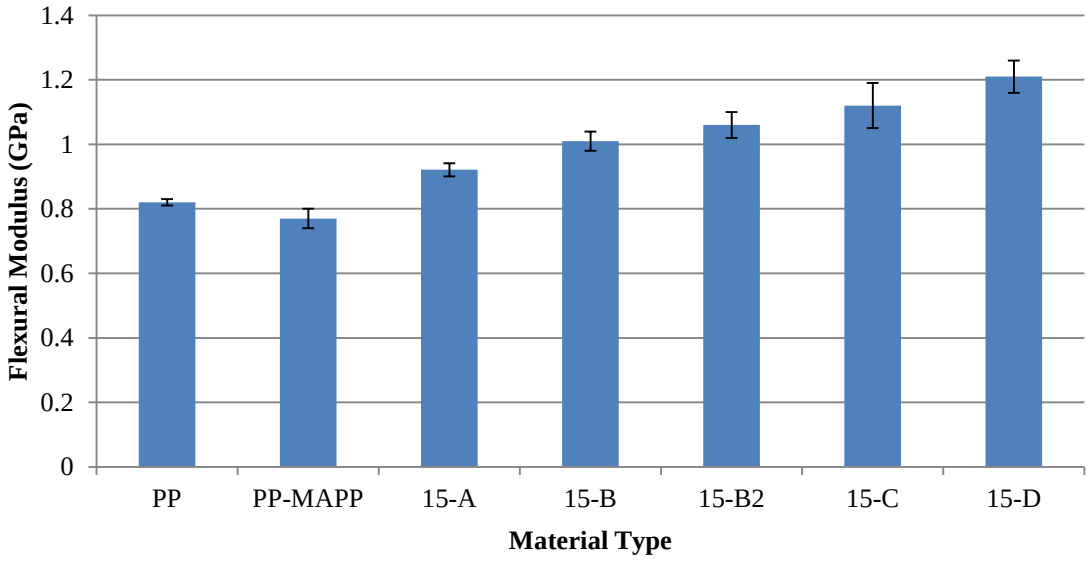

Figure 13. Flexural modulus of 15 wt. % hemp fiber reinforced PP composite variances. (A-untreated, B-5 wt. % NaOH, B2-10 wt. % NaOH, C-5 wt. % MAPP and D-5 wt. % NaOH + 5 wt. % MAPP)

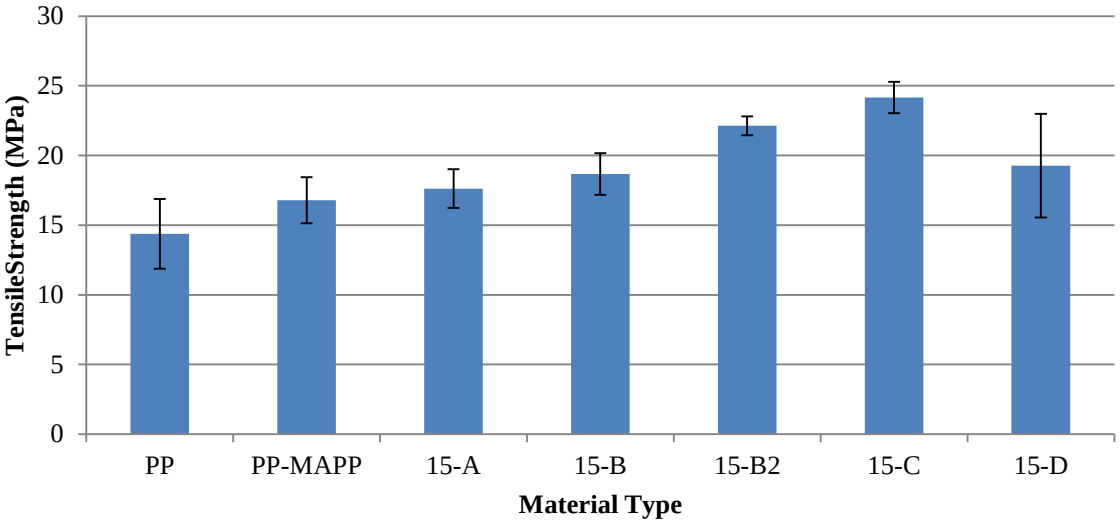

Figure 14. Tensile strength of 15 wt. % hemp fiber reinforced PP composite variances. (A-untreated, B-5 wt. % NaOH, B2-10 wt. % NaOH, C-5 wt. % MAPP and D-5 wt. % NaOH + 5 wt. % MAPP)

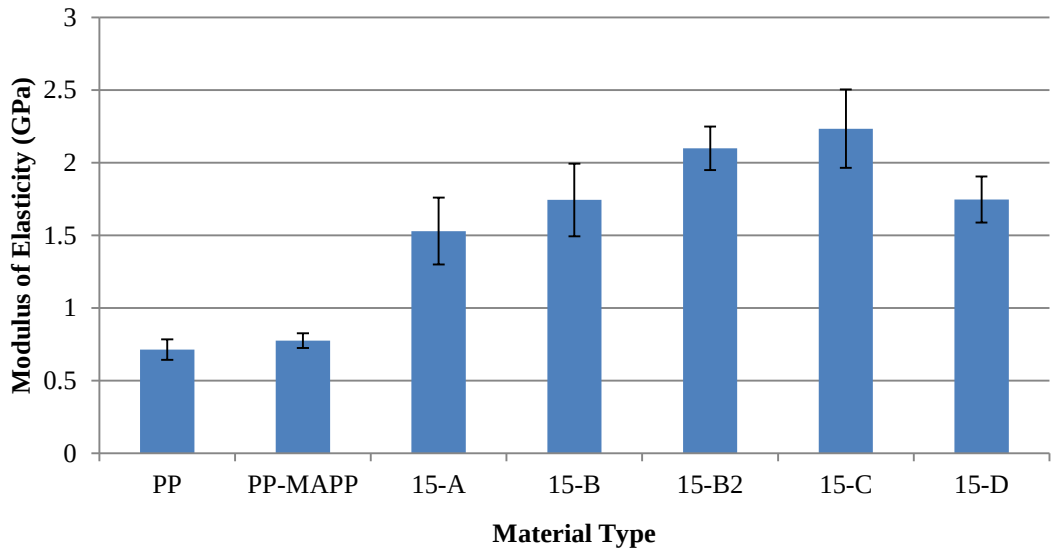

Figure 15. Modulus of elasticity of 15 wt. % hemp fiber reinforced PP composite variances. (A-untreated, B-5 wt. % NaOH, B2-10 wt. % NaOH, C-5 wt. % MAPP and D-5 wt. % NaOH + 5 wt. % MAPP)

15 wt. % Composite Surface Fracture Analysis

The SEM images in Figure 16 show the fracture surfaces of the 15 wt. % hemp fiber reinforced PP composites. Figure 16a shows 15-A with poor fiber-matrix interfacial adhesion. Several fiber breakages and some fiber pullout/debonding were evident. The protruding hemp fibers with the gaps around the fiber indicated poor bonding of the PP to the fibers. Both 15-B and 15-B2 showed an improvement of the bonding between fiber and matrix as shown in Figures 16b and c, but there were still space between the fiber and matrix. Figure 16d shows 15-C with the best fiber-matrix interfacial adhesion. The PP adhered to the surface of the hemp fibers without any gaps present. There was less damage on the fibers than the 15-A, 15-B and 15-B2. MAPP addition greatly improved the fiber-matrix adhesion thus increasing the mechanical properties as shown before. Figure 16e shows 15-D having several fiber pullouts and some poor interfacial bonding.

These results coincided with the poor tensile property data. Without chemical modifications or coupling agent additives to hemp fibers, the interfacial bonding between fiber and matrix was poor and lowered the mechanical properties of the composite.

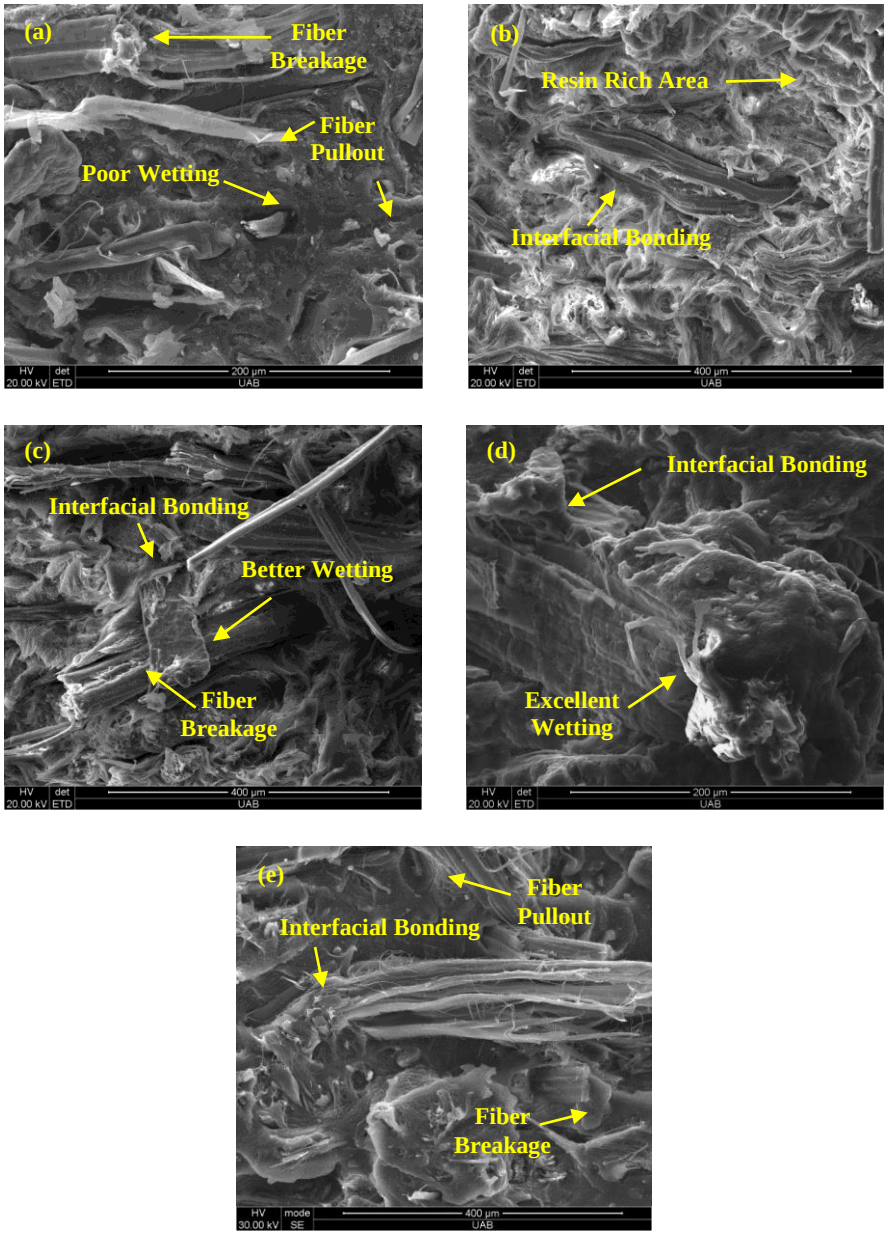

Figure 16. SEM images of 15 wt. % hemp fiber reinforced PP composite fiber fracture surfaces of (a) 15-A, (b) 15-B, (c) 15-B2, (d) 15-C and (e) 15-D. (A-untreated, B-5 wt. % NaOH, B2-10 wt. % NaOH, C-5 wt. % MAPP and D-5 wt. % NaOH + 5 wt. % MAPP)

Fiber Weight Percentage Comparison

As stated in the Compound-Extrusion Processing section, the 15 wt. % hemp fiber and 30 wt. % hemp fiber have different factor values for processing within the twin screw extruder. Due to the size limitation of the twin screw extruder, the maximum weight percentage that the twin screw can handle was 30 wt. % by changing the factor values mentioned in Table 8. Since there were several preliminary variances, the 30 wt. % fiber variances were minimized into four sets: 30-A, 30-B, 30-C and 30-D. The untreated set was selected to act as the control to compare properties against. Seeing as there was not a considerable difference in mechanical properties between the 5 wt. % and 10 wt. % NaOH, the 5 wt. % NaOH was chosen in consideration of cost and processing time. The 5 wt. % MAPP variance was chosen because it produced the best properties. The combination of NaOH treatment and MAPP coupling agent was selected to observe if there would be any significant increase in properties.

Only flexural and tensile properties were analyzed for the weight percentage comparison. Figures 17-20 compare the PP, 15 wt. % and 30 wt. % hemp fiber reinforced PP composites flexural and tensile strength and modulus. 30-A and 30-B variances did not have a significant increase in properties when the weight percentage increased as was evident in the samples with MAPP addition. As was shown with the 15 wt. % fiber data, 30-C overall had the best results. 30-C had a 40 %, 70 %, 32 % and 27 % increase, respectively, for the flexural strength and modulus and tensile strength and modulus compared to 15-C. In addition, 30-C had a 91 %, 132 %, 122 % and 297 % increase, respectively, for the flexural strength and modulus and tensile strength and modulus compared to PP.

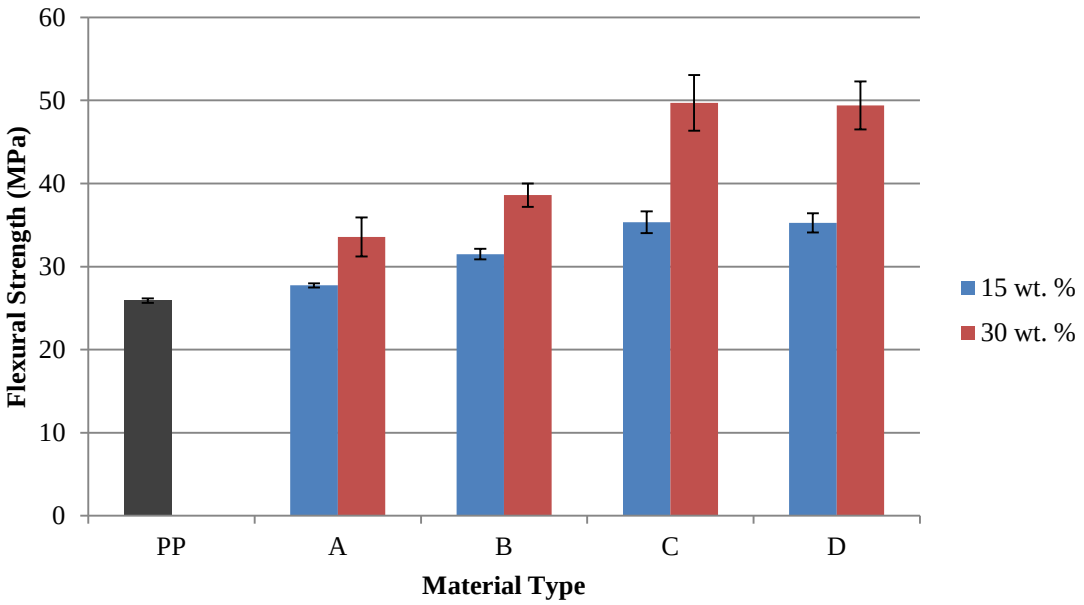

Figure 17. Flexural strength comparison of PP, 15 wt. % and 30 wt. % hemp fiber reinforced PP composites. (A-untreated, B-5 wt. % NaOH, C-5 wt. % MAPP and D-5 wt. % NaOH + 5 wt. % MAPP)

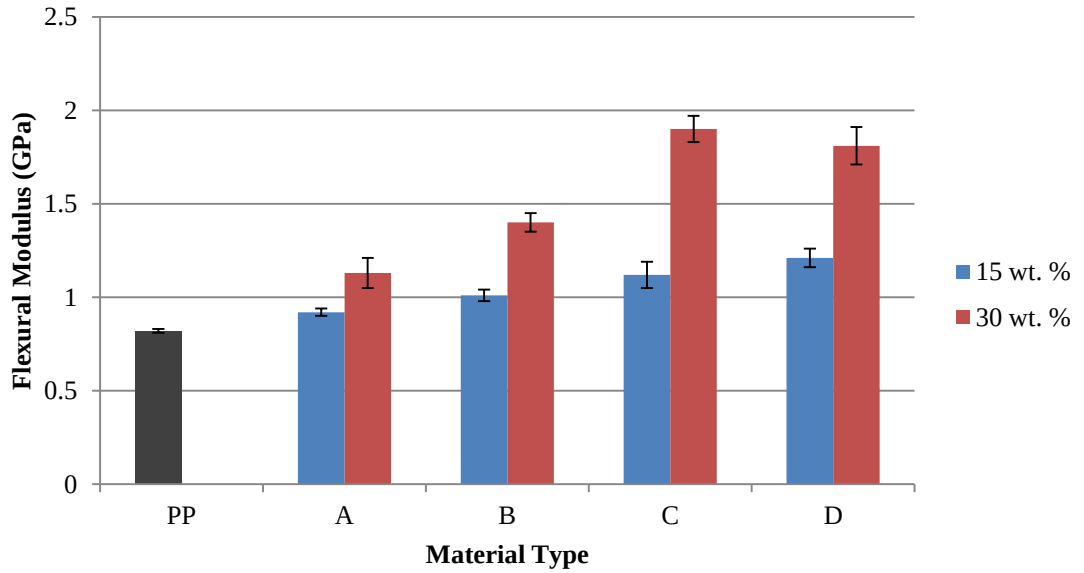

Figure 18. Flexural modulus comparison of PP, 15 wt. % and 30 wt. % hemp fiber reinforced PP composites. (A-untreated, B-5 wt. % NaOH, C-5 wt. % MAPP and D-5 wt. % NaOH + 5 wt. % MAPP)

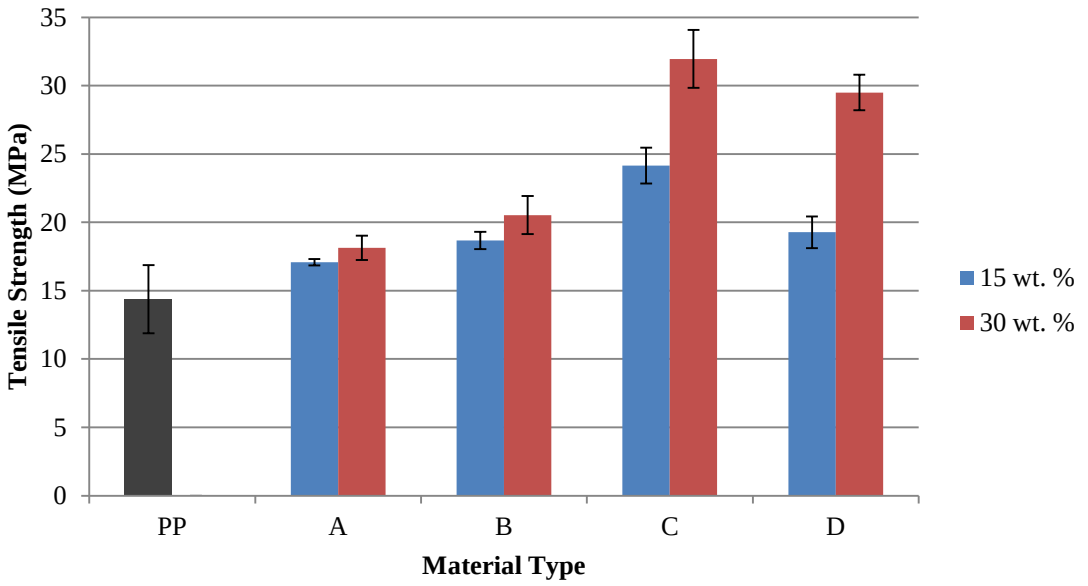

Figure 19. Tensile strength comparison of PP, 15 wt. % and 30 wt. % hemp fiber reinforced PP composites. (A-untreated, B-5 wt. % NaOH, C-5 wt. % MAPP and D-5 wt. % NaOH + 5 wt. % MAPP)

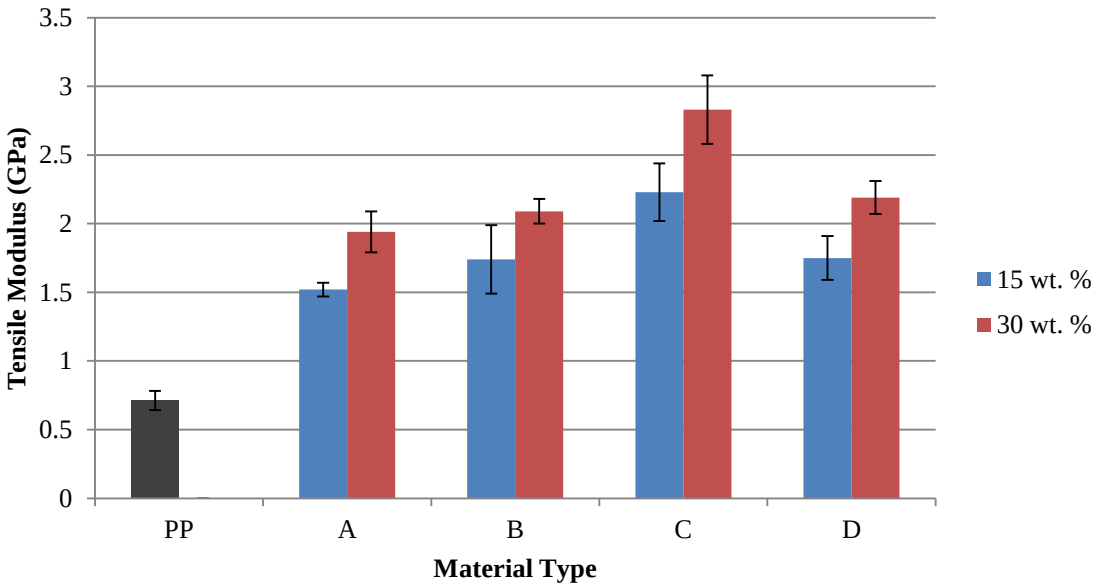

Figure 20. Tensile modulus comparison of PP, 15 wt. % and 30 wt. % hemp fiber reinforced PP composites. (A-untreated, B-5 wt. % NaOH, C-5 wt. % MAPP and D-5 wt. % NaOH + 5 wt. % MAPP)

30 wt. % Composite Surface Fracture Analysis

Figure 21 shows the SEM images of the fracture surfaces of the 30 wt. % hemp fiber reinforced PP composites. Both 30-A and 30-B specimens had several fiber pullouts and poor interfacial bonding where fiber breakage occurred as shown in Figures 21a-b. The specimens containing MAPP had excellent interfacial bonding and wetting of the fibers as shown in Figures 21c-d. There were no gaps between the fiber and matrix on the interface where fiber pullout and breakage were evident. This phenomenon coincided with the noticeable increase in mechanical properties. Fiber defibrillation, breakage of the fiber bundles, was evident in all the variances, whereas in the 15 wt. % batch there was barely or no fiber defibrillation due to higher fiber weight percentage loading. According to Cao et al., fiber treatment causes defibrillation which increases the contact area between fiber and matrix leading to better mechanical properties [97].

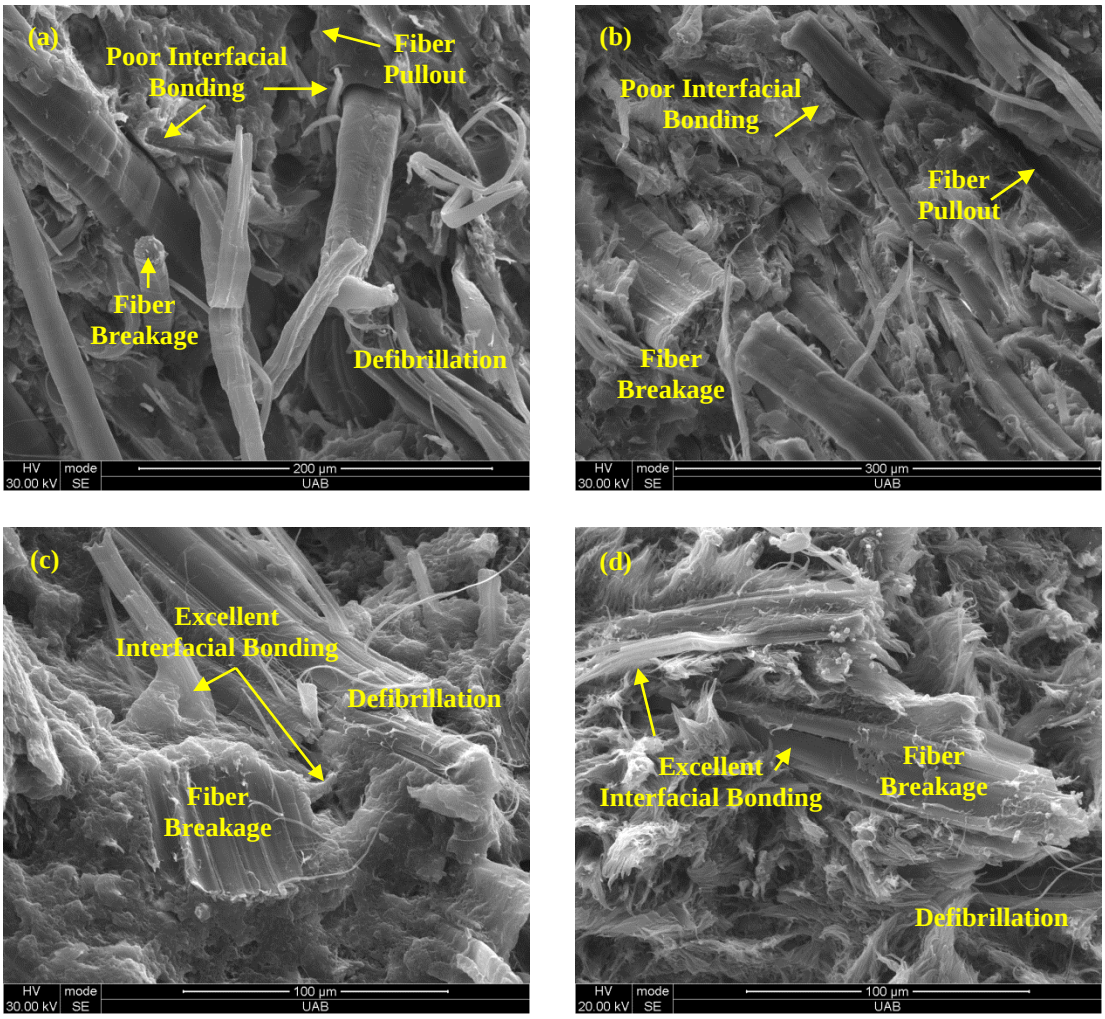

Figure 21. SEM images of 30 wt. % hemp fiber reinforced PP composite fiber fracture surfaces of (a) 30-A, (b) 30-B, (c) 30-C and (d) 30-D. (A-untreated, B-5 wt. % NaOH, C-5 wt. % MAPP and D-5 wt. % NaOH + 5 wt. % MAPP)

Hygrothermal Comparison

Accelerated Water Absorption

Natural fibers exhibit considerable moisture uptake due to their hydrophilic nature causing composites to decrease in mechanical properties and limiting application usage. Water absorption in the matrix; however, is negligible and has been studied by several researchers [73, 74, 98]. Figures 22-24 below show the accelerated water absorption

curves at 40 °C, where percentage of water absorbed is plotted against the square root of time (hours). All samples from each testing set steadily increased in water absorption until it reached between 400 to 900 hours where it plateaued to full saturation. Water absorption percentages from all testing sets are summarized in Table 13. 30-X-A had the highest water absorption percentage. From previous SEM images of the fracture surfaces, the high water absorption is caused from the poor fiber-matrix bonding in the interface region. Moisture is absorbed into the free volume space present in the structure where the microcracks/gaps allow the moisture to flow and store water within the cracks/gaps [80]. Both the 30-X-C and 30-X-C followed the same trend and had minimal difference in saturation value, which both were approximately 20-23 % less than the untreated sample. The addition of a chemical treatment and/or coupling agent has been well documented to reduce the water uptake as shown in this research due to the better interfacial bonding. Overall, the 30-X-D had the least water absorption, which was 30 % less than 30-A and about 10-20 % less than the 30-X-C.

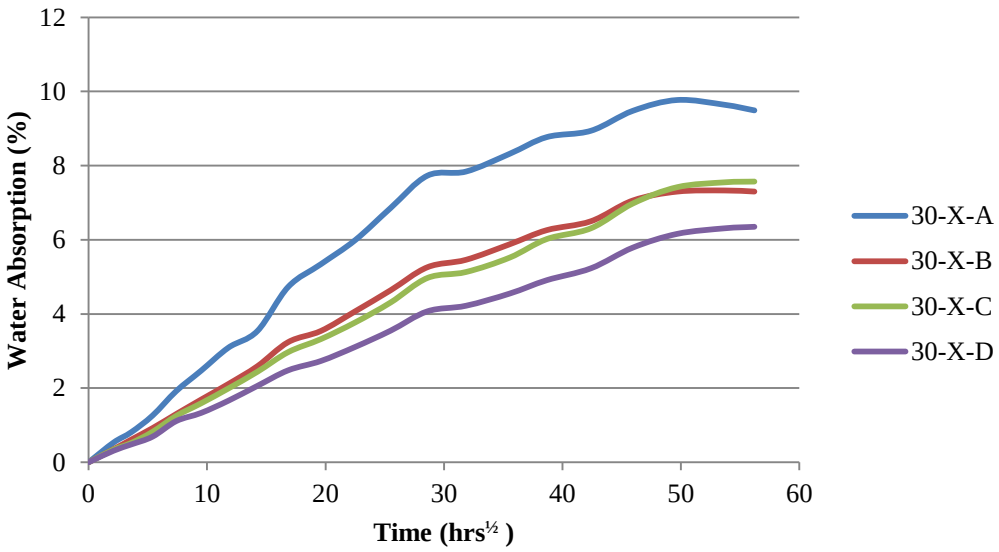

Figure 22. Accelerated moisture uptake analysis on flexural samples at 40 °C. (A-untreated, B-5 wt. % NaOH, C-5 wt. % MAPP and D-5 wt. % NaOH + 5 wt. % MAPP)

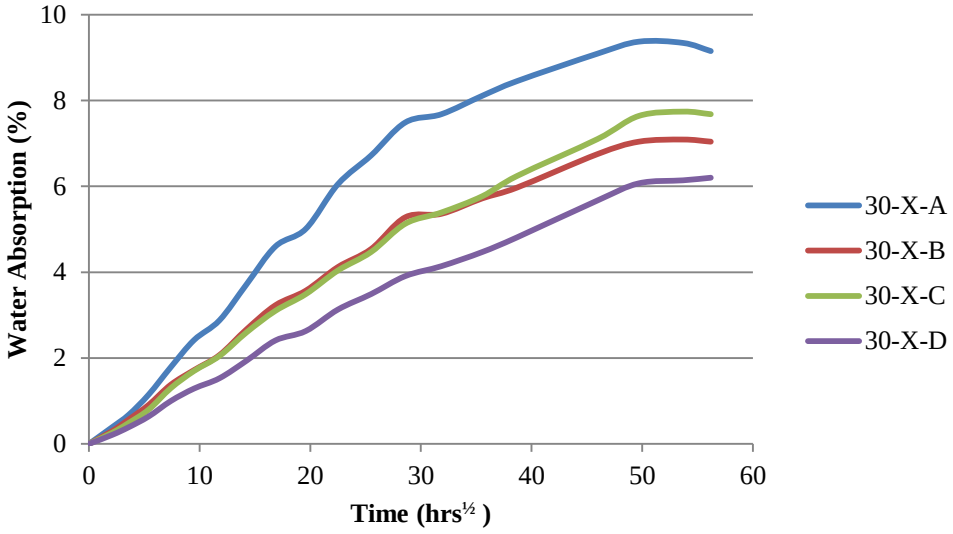

Figure 23. Accelerated moisture uptake analysis on tensile samples at 40 °C. (A-untreated, B-5 wt. % NaOH, C-5 wt. % MAPP and D-5 wt. % NaOH + 5 wt. % MAPP)

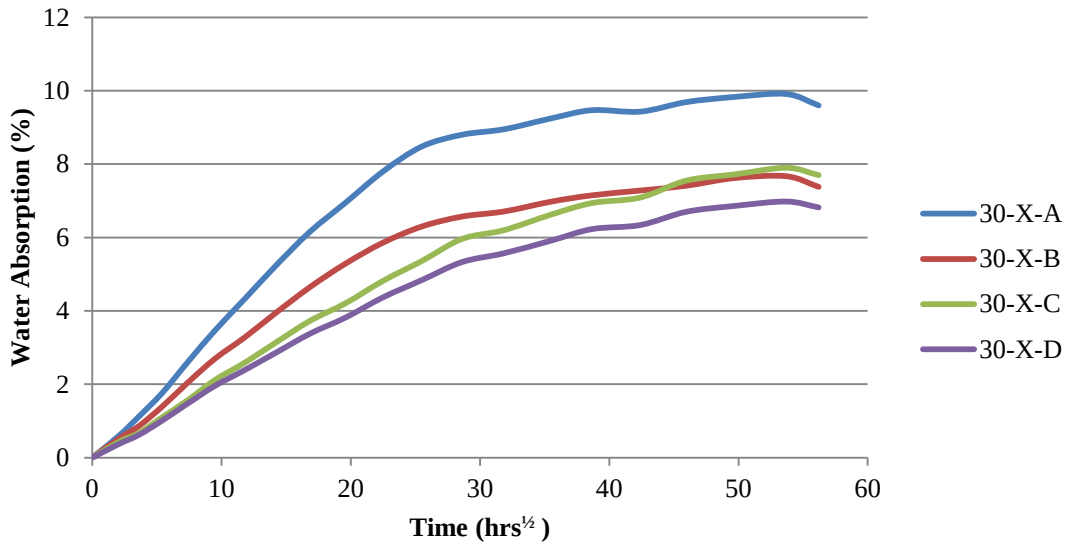

Figure 24. Accelerated moisture uptake analysis on izod impact samples at 40 °C. (A-untreated, B-5 wt. % NaOH, C-5 wt. % MAPP and D-5 wt. % NaOH + 5 wt. % MAPP)

Table 13

Equilibrium accelerated moisture absorption percentage comparison

Sample	Sample ID	Flexural	Tensile	Izod Impact
30-X-A	Untreated	9.49	9.15	9.60
30-X-B	5 wt. % NaOH	7.30	7.04	7.38
30-X-C	5 wt. % MAPP	7.57	7.68	7.70
30-X-D	5 wt. % NaOH + 5 wt. % MAPP	6.35	6.20	6.82

Mechanical properties comparison after accelerated aging conditions. Figures 25-28 show the effects of the accelerated moisture uptake on the flexural and tensile properties after saturation as-wet and re-dried samples. The 30-X-A and 30-X-B specimens did not have a considerable decrease in flexural and tensile strength as the 30-

X-C and 30-X-D specimens presented. On the other hand, the modulus of elasticity values of 30-X-C-W and 30-X-D-W showed the greatest reduction in all properties having between 15-50 % decrease from 30-X-C-O and 30-X-D-O. Out of all the variances, 30-X-C-W had the biggest decline in all properties; however, it had the greatest recovery percentage (30-X-C-RD) ranging between 10-20 %. The mechanical properties values of the 30-X-C-W and 30-X-C-D still had better properties than 30-X-A-O, except for the tensile modulus where 30-X-C-W and 30-X-C-RD only had higher modulus on both conditioned 30-X-A specimens.

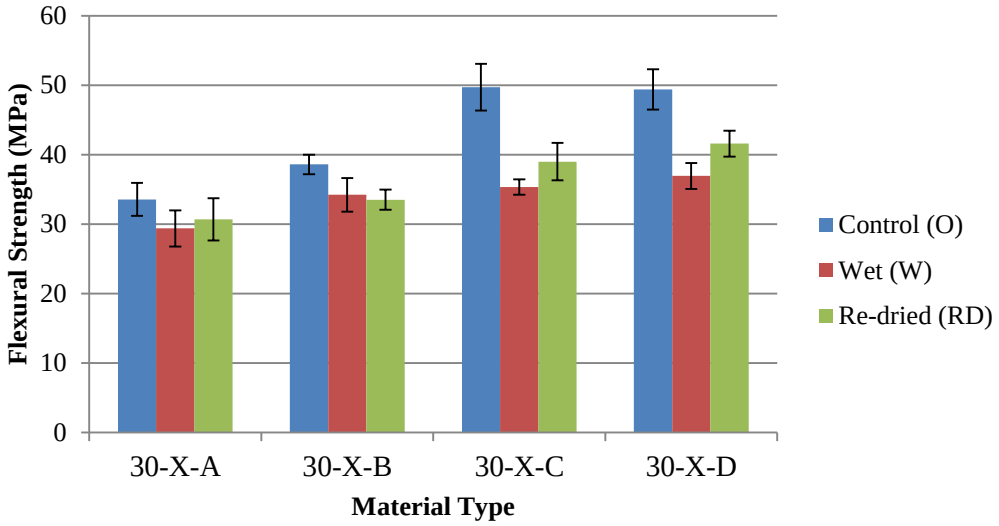

Figure 25. Flexural strength comparison of control, wet and re-dried samples after accelerated moisture uptake. (A-untreated, B-5 wt. % NaOH, C-5 wt. % MAPP and D-5 wt. % NaOH + 5 wt. % MAPP)

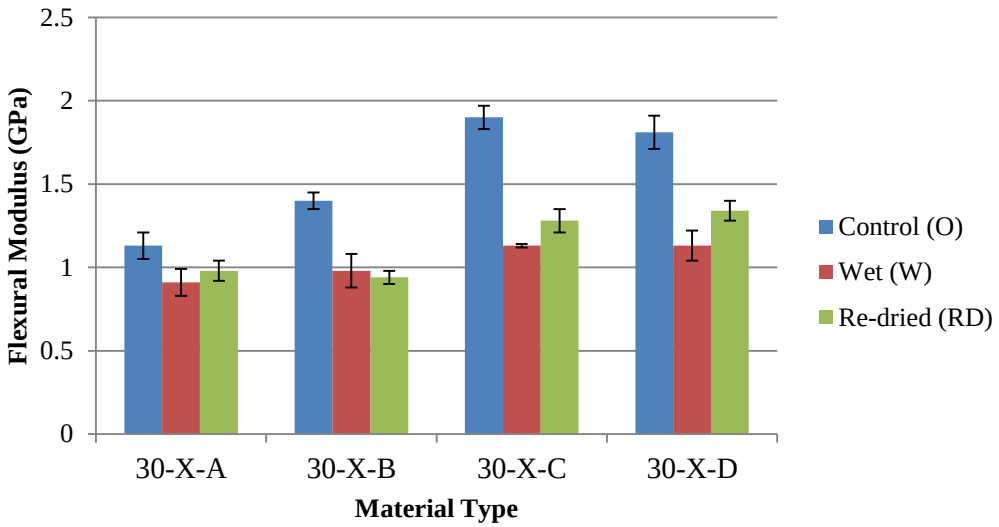

Figure 26. Flexural modulus comparison of control, wet and re-dried samples after accelerated moisture uptake. (A-untreated, B-5 wt. % NaOH, C-5 wt. % MAPP and D-5 wt. % NaOH + 5 wt. % MAPP)

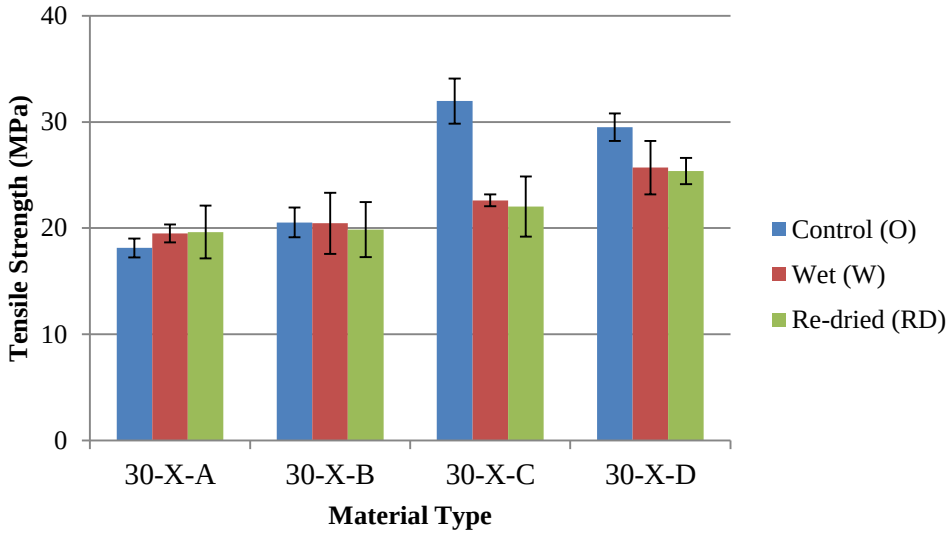

Figure 27. Tensile strength comparison of control, wet and re-dried samples after accelerated moisture uptake. (A-untreated, B-5 wt. % NaOH, C-5 wt. % MAPP and D-5 wt. % NaOH + 5 wt. % MAPP)

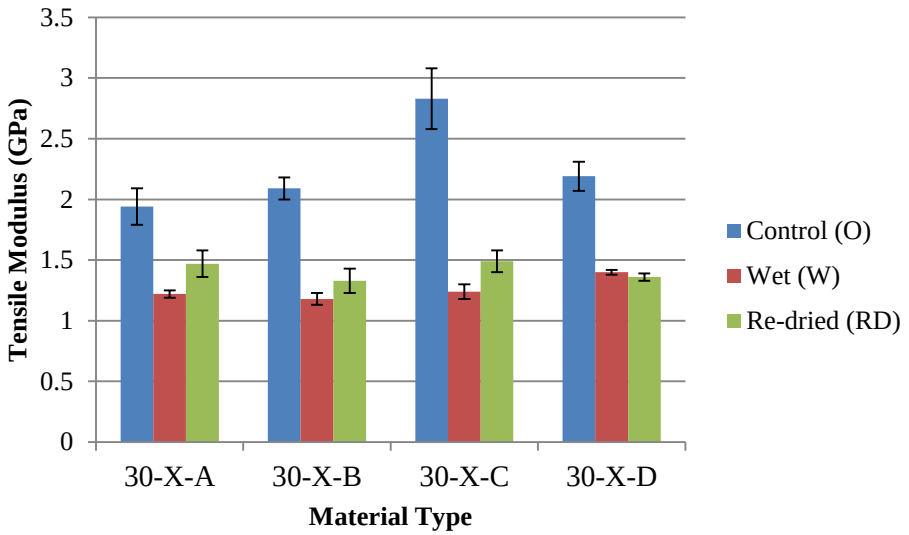

Figure 28. Tensile modulus comparison of control, wet and re-dried samples after accelerated moisture uptake. (A-untreated, B-5 wt. % NaOH, C-5 wt. % MAPP and D-5 wt. % NaOH + 5 wt. % MAPP)

The decrease in mechanical properties can be attributed to the swelling of the fibers as shown in Figure 29. Fiber swelling and color fading of the samples were noticed within two weeks of the specimens being fully immersed in water. Moisture buildup in the fiber cell wall can lead to a plasticization effect, where interfacial shear stress is developed when the osmotic pressure increases due to the fiber swelling that causes adhesive debonding [73]. Panthapulakkal et. al reported that prolonged interaction with water in natural fiber composites can result in an irreversible damage to the fiber and fiber-matrix interface, which decreases the properties of the composite [74]. This damage is the reason why there was not a full recovery of the properties when the samples were re-dried.

Figure 29. Control tensile sample (AT3) compared to accelerated moisture uptake sample (AT10) for hemp fiber swelling and discoloration of composite.

Table 14 shows the izod impact strength properties. The addition of a chemical treatment to the fiber and/or a coupling agent in the control samples proved to increase the impact strength of the 30-X-A-O by 5-15 %. Huda et al. reported that treated natural fiber reinforced composites improved the impact strength due to better interfacial adhesion that provided an effective resistance to crack propagation during impact tests [99].

Table 14

Impact strength (kJ/m^2) with standard deviation of accelerated moisture absorption set

Sample	Sample ID	Control (O)	Wet (W)	Re-dried (RD)
30-X-A	Untreated	5.09 ± 0.69	8.46 ± 1.30	6.58 ± 0.84
30-X-B	5 wt. % NaOH	5.30 ± 1.19	6.77 ± 1.48	6.95 ± 1.33
30-X-C	5 wt. % MAPP	5.80 ± 0.60	5.89 ± 1.23	6.74 ± 1.35
30-X-D	5 wt. % NaOH + 5 wt. % MAPP	5.52 ± 0.47	6.30 ± 0.99	6.13 ± 0.85

All samples showed an increase in properties when the samples were immediately tested after reaching full saturation (as-wet samples) except for the 30-X-C set which stayed constant. The 30-X-A-W samples had the highest increase of 66 % from 5.09 kJ/m^2 to 8.46 kJ/m^2. The maximum moisture absorption made the hemp fibers more flexible, tougher than the brittle nature of natural fibers, thus causing an increase in impact properties. The impact strength of a composite is directly related to the toughness of the material. Higher impact strength properties were shown in 30-X-A-W and 30-X-B-W samples than 30-X-C-W and 30-X-D-W samples due to the fiber failure mode. As was shown in several SEM images, the 30-A and 30-B samples showed poor interfacial adhesion with fiber pullout throughout the fracture surfaces while 30-C and 30-D samples showed better interfacial adhesion and fiber breakage throughout the fracture surfaces.

Alimuzzaman et al. investigated impact strength of flax fiber reinforced PLA composites that at the fracture surface, flax fibers were broken in the case of a more brittle sample, whereas fibers were pulled out from the surface in the case of less brittle samples [100]. Weaker bonds lead to better impact strength due to the energy absorption when fibers are pulled from the matrix than very strong bonding which can cause sudden failure [101, 102]. The re-dried samples either stayed constant or dropped in impact strength. Once the fibers were dry again, they returned to their brittle nature, but still had better properties than the control set due to the weaker bonds created when the fibers were swelled.

Realistic Aging Conditions

Figures 30-32 show the realistic environment water absorption aging at 40 °C with 65 % humidity for 841 hours. All samples from each testing set slowly increased in water absorption percentage. Table 15 summarizes the water absoprtion for the realistic condition. 30-R-A specimens did not reach 1 % water absorption after 841 hours whereas 30-X-A set reached 1 % water absorption at approximately 25 hours.

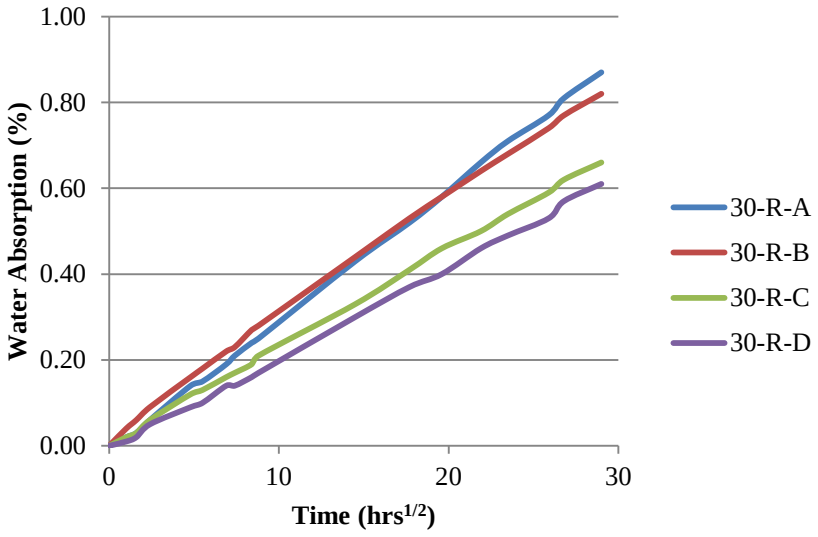

Figure 30. Realistic moisture uptake analysis on flexural samples at 40 °C at 65 % humidity. (A-untreated, B-5 wt. % NaOH, C-5 wt. % MAPP and D-5 wt. % NaOH + 5 wt. % MAPP)

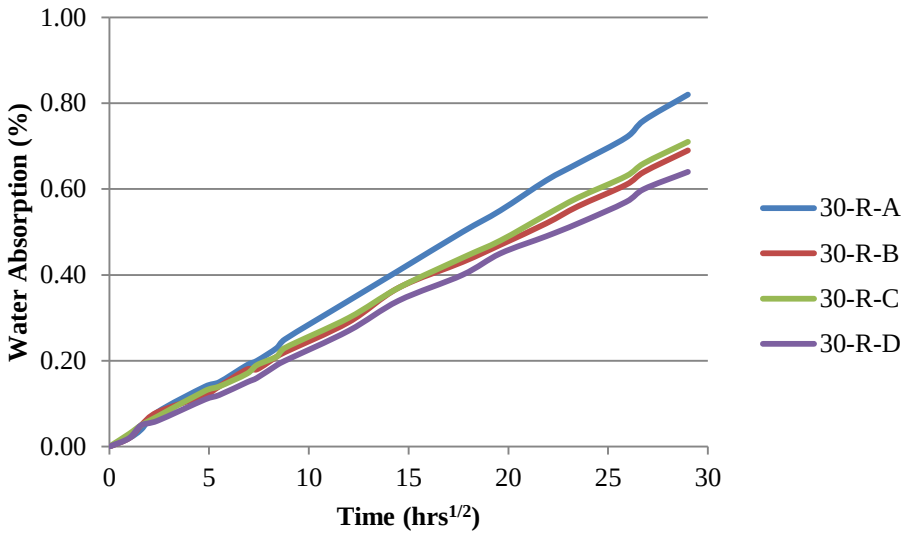

Figure 31. Realistic moisture uptake analysis on tensile samples at 40 °C at 65 % humidity. (A-untreated, B-5 wt. % NaOH, C-5 wt. % MAPP and D-5 wt. % NaOH + 5 wt. % MAPP)

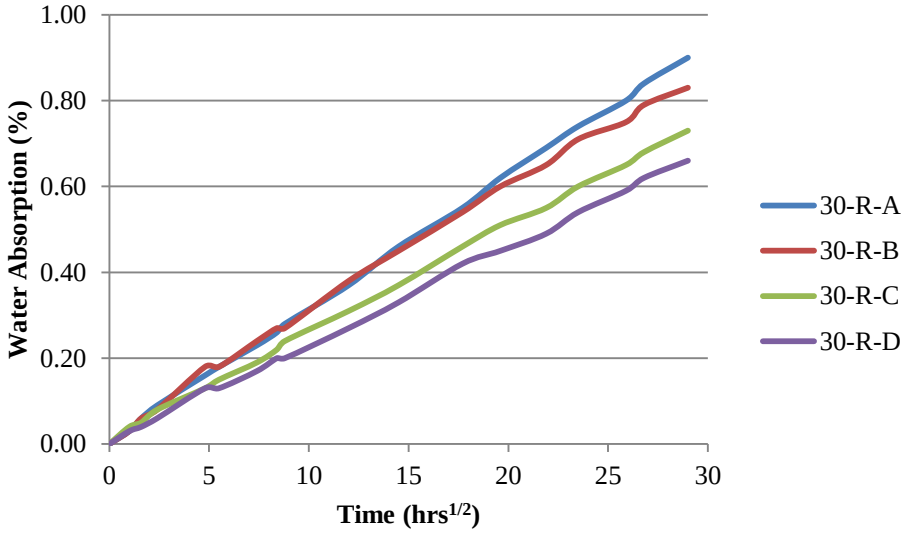

Figure 32. Realistic moisture uptake analysis on izod impact samples at 40 °C at 65 % humidity. (A-untreated, B-5 wt. % NaOH, C-5 wt. % MAPP and D-5 wt. % NaOH + 5 wt. % MAPP)

Table 15

Equilibrium realistic moisture absorption percentage comparison

Sample	Sample ID	Flexural	Tensile	Izod Impact
30-R-A	Untreated	0.87	0.82	0.90
30-R-B	5 wt. % NaOH	0.82	0.69	0.83
30-R-C	5 wt. % MAPP	0.66	0.71	0.73
30-R-D	5 wt. % NaOH + 5 wt. % MAPP	0.61	0.64	0.66

Mechanical properties comparison after realistic aging conditions. Figures 33-36 and Table 16 show the flexural, tensile and izod impact properties of the realistic conditioned samples. All the mechanical properties did not show a significant increase nor change in properties due to the minimal water uptake. In addition, the samples did not show any indication of fiber swelling or color change as shown in Figure 37. No change in properties nor any physical change of the samples indicate that there was very little or no damage in the fiber, matrix and fiber-matrix interfacial adhesion

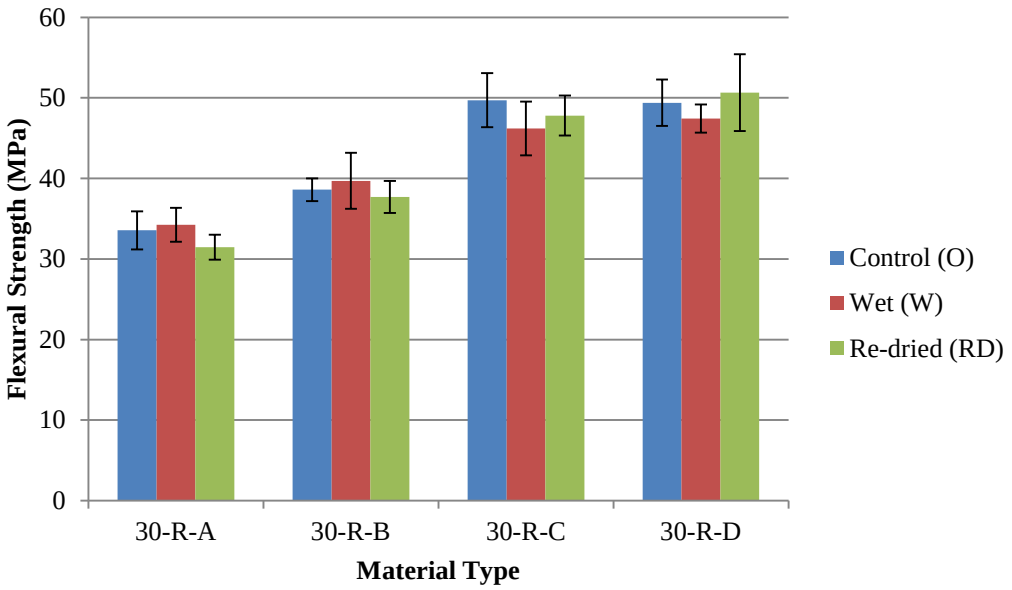

Figure 33. Flexural strength comparison of control, wet and re-dried samples after realistic moisture uptake. (A-untreated, B-5 wt. % NaOH, C-5 wt. % MAPP and D-5 wt. % NaOH + 5 wt. % MAPP)

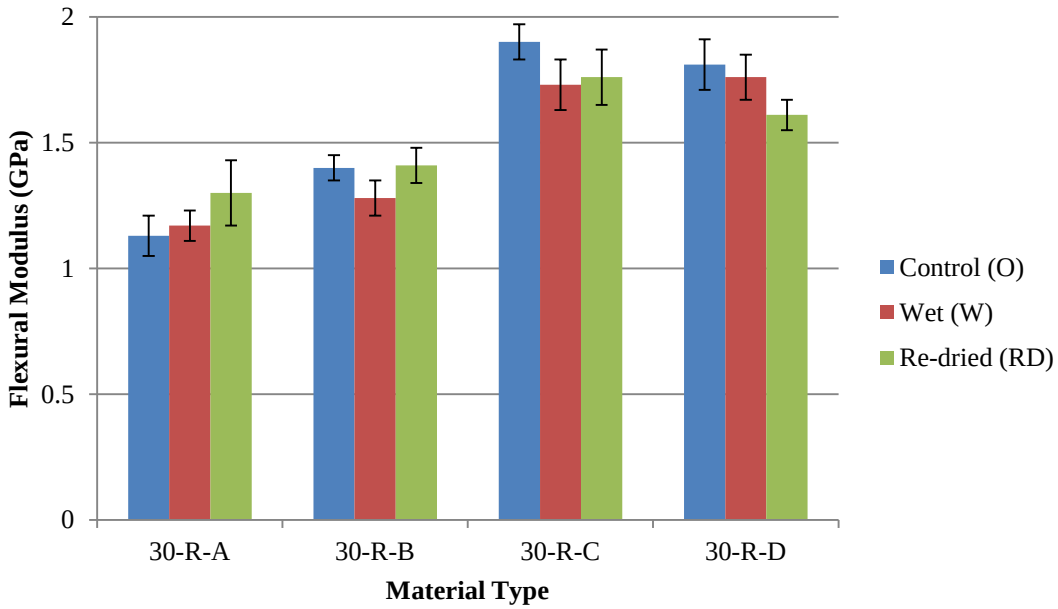

Figure 34. Flexural modulus comparison of control, wet and re-dried samples after realistic moisture uptake. (A-untreated, B-5 wt. % NaOH, C-5 wt. % MAPP and D-5 wt. % NaOH + 5 wt. % MAPP)

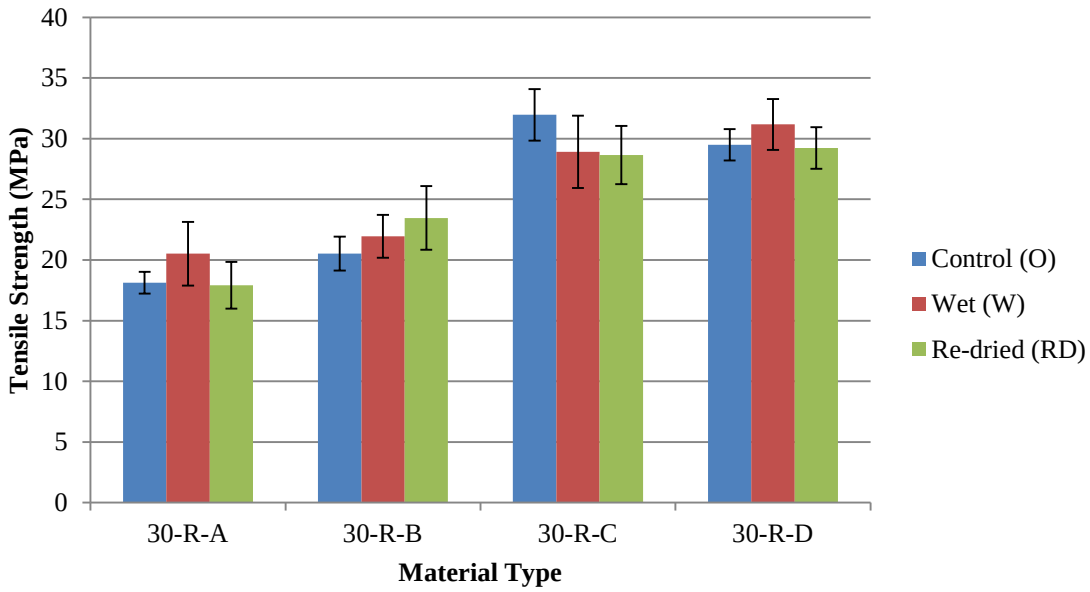

Figure 35. Tensile strength comparison of control, wet and re-dried samples after realistic moisture uptake. (A-untreated, B-5 wt. % NaOH, C-5 wt. % MAPP and D-5 wt. % NaOH + 5 wt. % MAPP)

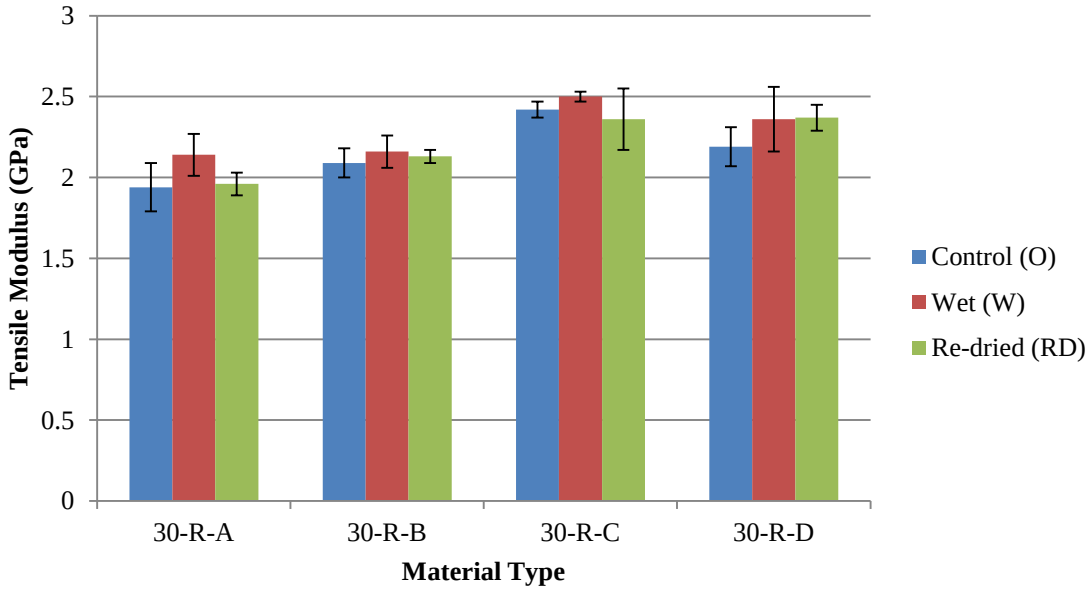

Figure 36. Tensile modulus comparison of control, wet and re-dried samples after realistic moisture uptake. (A-untreated, B-5 wt. % NaOH, C-5 wt. % MAPP and D-5 wt. % NaOH + 5 wt. % MAPP)

Table 16

Impact strength (kJ/m^2) with standard deviation of realistic moisture absorption set

Sample	Sample ID	Control (O)	Wet (W)	Re-dried (RD)
30-R-A	Untreated	5.09 ± 0.69	5.75 ± 0.92	6.10 ± 1.14
30-R-B	5 wt. % NaOH	5.30 ± 1.19	5.38 ± 2.23	4.98 ± 0.41
30-R-C	5 wt. % MAPP	5.80 ± 0.60	6.03 ± 0.59	6.10 ± 0.37
30-R-D	5 wt. % NaOH + 5 wt. % MAPP	5.52 ± 0.47	5.94 ± 0.46	6.25 ± 0.60

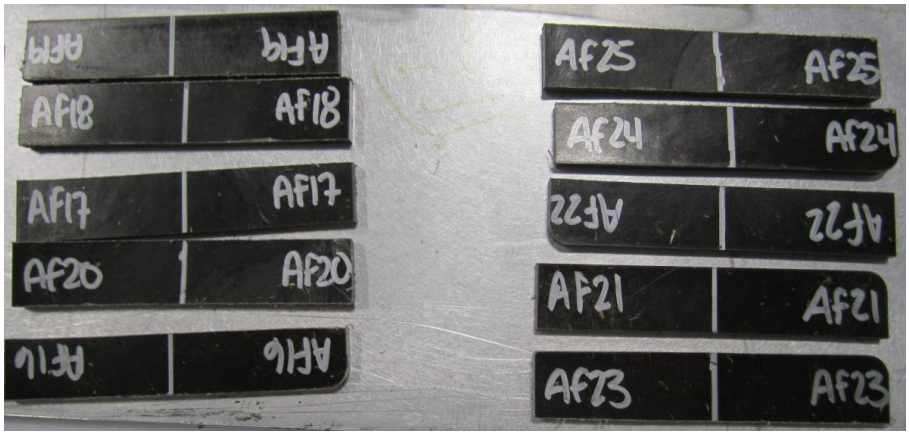

Figure 37. Flexural untreated samples after realistic aging with no indication of hemp fiber swelling and discoloration of composite.

UV Exposure Analysis

The visual appearance of the 30 wt. % hemp fiber reinforced PP changed as a result of UV exposure. The color of the exposed surface changed from a dark brown to a chalky white color as shown in Figures 38 and 39. The 500 hours and 1,000 hours conditioned samples did not have any physical difference between each other. Both had

the same chalky white color. Powder like material was flaking off the composite indicating matrix damage. Extensive fiber exposure can be seen on the composite surface.

Figure 38. Flexural samples exposed to UV radiation for 500 hours.

Figure 39. Flexural samples exposed to UV radiation for 1,000 hours.

Flexural Property Comparison

Figures 40 and 41 show the flexural strength and modulus comparison of the control set versus the 500 and 1,000 hrs UV exposed samples. The 500 and 1,000 hrs set did not have a considerable difference in property change between the two sets. 30-C had the highest reduction in strength and modulus, respectively, by 27 % and 29 % from 30-A. Even with the decrease in properties, 30-C UV exposed samples had either the same or better properties than both the 30-A and 30-B control samples.

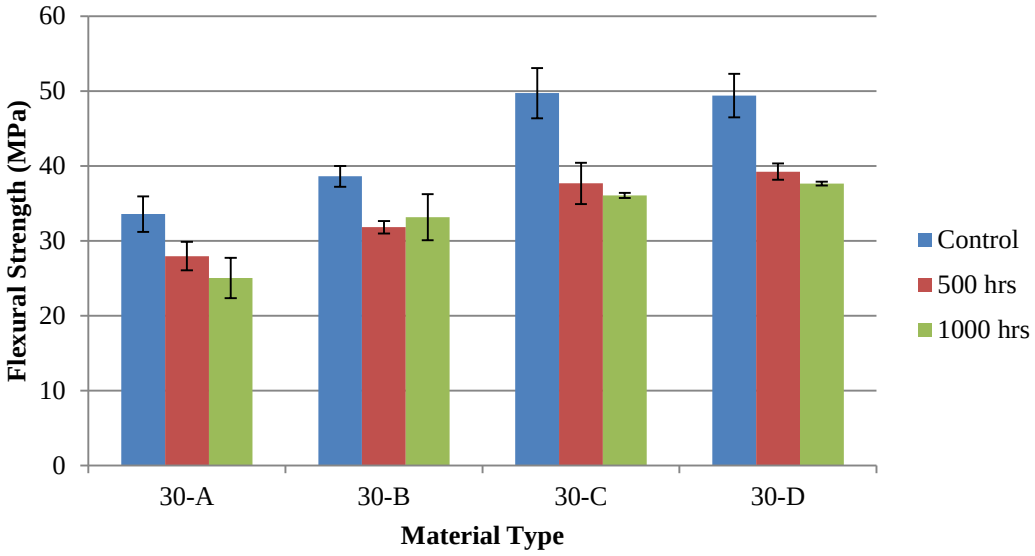

Figure 40. Flexural strength comparison of the control, 500 hrs UV exposed and 1,000 hrs UV exposed samples. (A-untreated, B-5 wt. % NaOH, C-5 wt. % MAPP and D-5 wt. % NaOH + 5 wt. % MAPP)

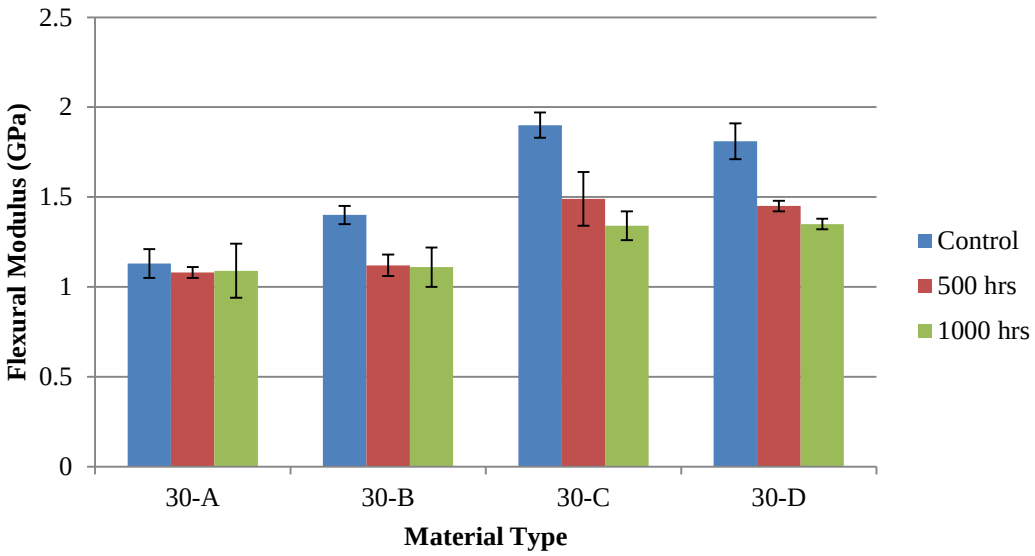

Figure 41. Flexural modulus comparison of the control, 500 hrs UV exposed and 1,000 hrs UV exposed samples. (A-untreated, B-5 wt. % NaOH, C-5 wt. % MAPP and D-5 wt. % NaOH + 5 wt. % MAPP)

The SEM images were taken on the surface and fracture surface of the 30-C UV exposed samples as shown in Figure 42. Mirco-cracks were formed after the samples were exposed to UV radiation, which caused the decrease in flexural properties. Figure 42b shows the gaps in the matrix and the flake-like pieces of the matrix that was mentioned prior. Fiber debonding on the outer surface was evident which also contributed to the lower properties. However, Figure 42c shows good interfacial bonding between fiber and matrix in the inner surface of the fractured samples. Goel reported that only a few hundred micrometers from the surface is degraded from the UV exposure while the inner surface of the composite remained unaffected in its modulus properties on LFTs (21 vol. % E-glass reinforced PP composites) [30].

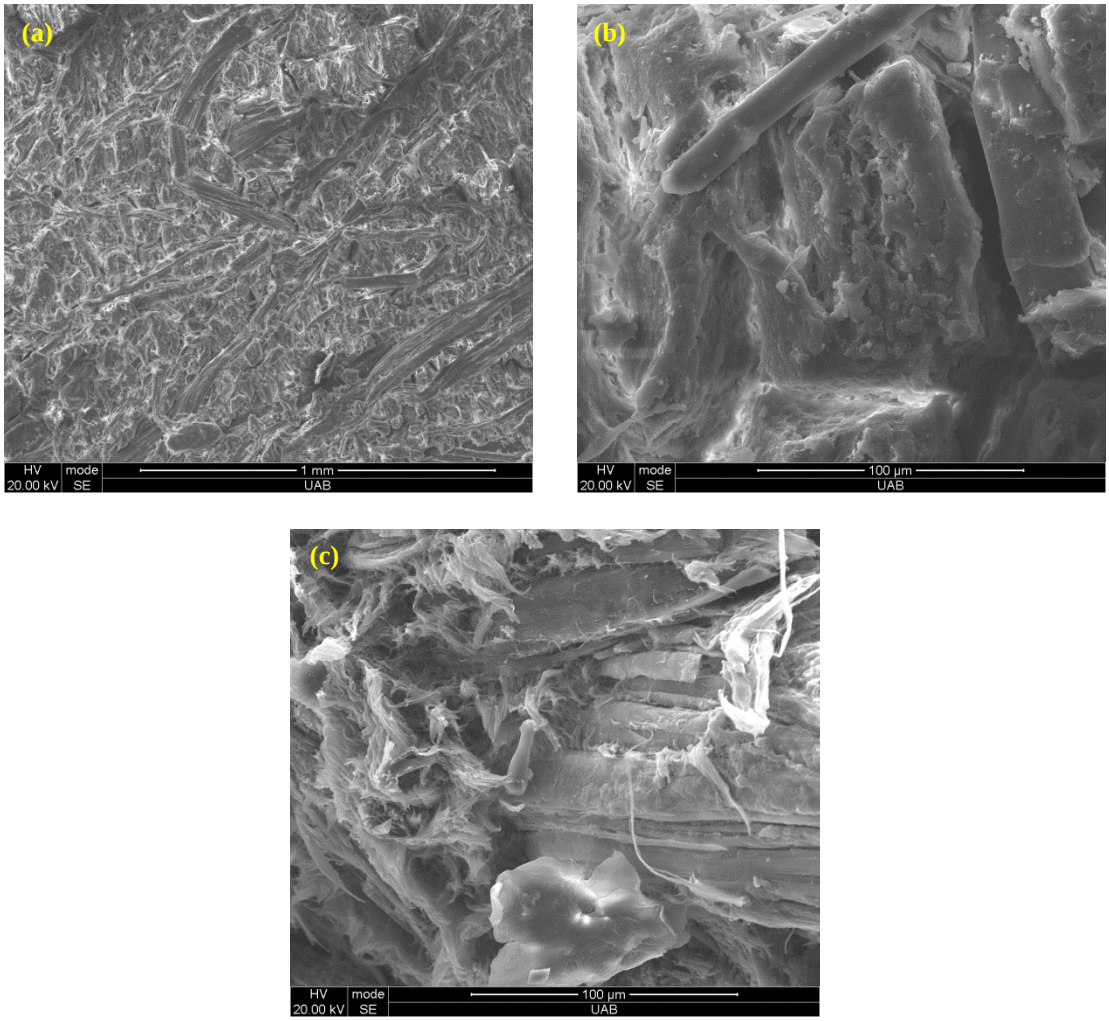

Figure 42. SEM images of 30-C (5 wt. % MAPP) UV exposed samples of (a, b) 500 hrs exposed surfaces and (c) 1,000 hrs exposed fracture surface.

Prototype Development: Duct Screen Cleaner

Background

MacDon Industries located in Winnipeg, Manitoba, Canada, is a family-owned manufacturer of harvesting equipment specializing in the production of pull-type and self-propelled windrowers and specialty and pick-up headers for combines for world

markets. Similar to other manufacturers and companies in Canada, MacDon is striving to become more eco-friendly and has an interest in using sustainable materials.

One of the components that was compatible with UAB's manufacturing capability was the duct-screen cleaner. The duct-screen cleaner acts as a secondary 'guard' to protect the engine from dust and debris. The mesh screens are the primary 'guard' that is located in front of the engine as shown in Figure 43. There are two duct-screen cleaners in the windrower tractors that rotate at 2 rpm, which collect the dust and debris through vacuum.

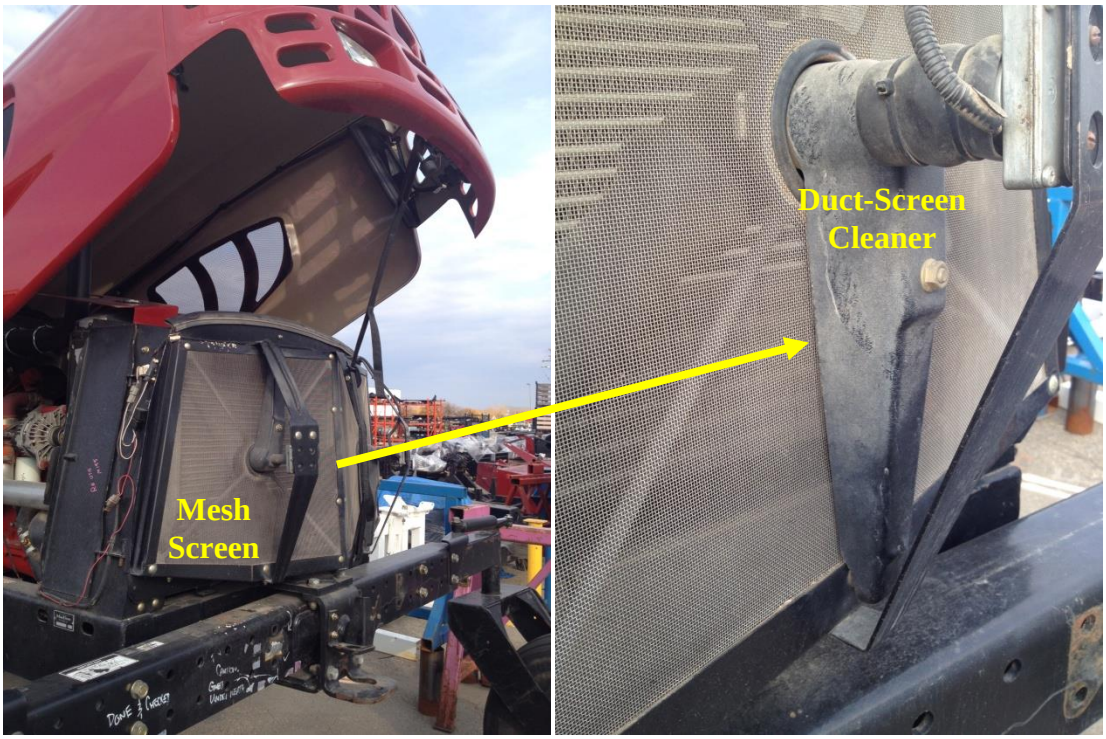

Figure 43. MacDon windrower tractor showing the mesh screens and duct-screen cleaner.

Original Manufacturing Method of the Duct-Screen Cleaner

MacDon did not have any specific requirements for the duct-screen cleaner, which allowed more flexibility in the design. The duct-screen cleaner was originally manufactured via thermoforming. The problem with this manufacturing method was that it did not have consistent form and definition of the component. For example, the arrow on the duct-screen cleaner was a blob rather than an arrow. Thus, the compression molding method presented in this research should alleviate these issues.

Extrusion-Compression Molding Method

Once the male and female tool die were machined, the two parts were bolted to an existing tool as shown in Figure 44. 30 wt. % hemp fiber reinforced PP composite with 5 wt. % MAPP out of all the variances had the overall desirable properties based on the mechanical and environmental properties, processing cost and carbon footprint. An extruded 30 wt. % hemp fiber reinforced PP composite with 5 wt. % MAPP charge of 45.7 mm was the minimum amount of material needed to fill the tool. The charge was placed 25.4 mm away from the radius end as shown in Figure 45 then compression molded. The duct-screen cleaner prototype was then trimmed of the excess flash, and the two holes for the vacuum setup were drilled. Figure 46 shows the successful duct-screen cleaner prototype with consistent form and definition that was not seen in the original manufacturing method.

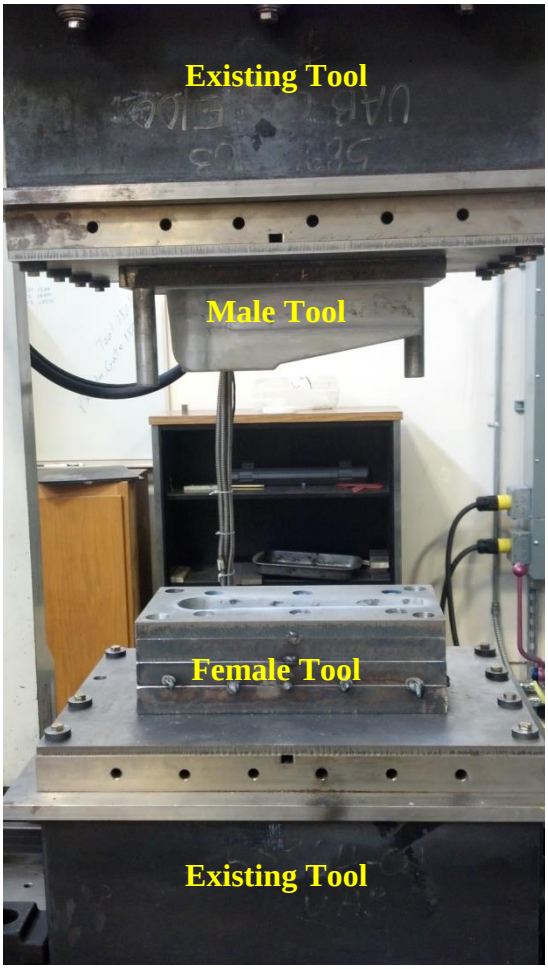

Figure 44. Male and female duct-screen cleaner tool bolted to an existing tool.

Figure 45. Extruded charge placed 25.4 mm away from the female tool radius end.

Figure 46. 30 wt. % hemp fiber reinforced PP composite with 5 wt. % MAPP duct-screen prototype via compounding-extrusion-compression molding manufacturing process.

CONCLUSIONS

Hemp Fiber Length and Aspect Ratio

This research focused on maintaining long fiber lengths to obtain high aspect ratio in an alternative thermoplastic manufacturing method via twin screw compounding-extrusion-compression molding process. The DOE analysis showed that after the twin screw compounding process, long fiber lengths, roughly 17.1 mm, were achieved. The twin screw extruding process was optimized from previous work by selecting the appropriate screws for the twin screw extruder, introducing a side stuffer for the fibers and designing a tape form die plate for minimal shearing and fiber degradation. The average hemp fiber length was 60 % of the average unprocessed length (25.4 mm) resulting in a high aspect ratio of 628 to achieve higher mechanical properties of the composite.

Fiber Treatment and Coupling Agent Characterization

Alkaline fiber treatment and/or the addition of a maleated coupling agent proved to increase the flexural and tensile properties and improve the interfacial adhesion between the fiber and matrix in hemp fiber reinforced PP composites. The addition of 5 wt. % MAPP with no chemical treatments had the best result overall as follows:

- 15 wt. % hemp fiber reinforced PP composite with 5 wt. % MAPP had a 37 %, 37 %, 68 % and 213 % increase in flexural strength and modulus and tensile strength and modulus compared to PP.

- 30 wt. % hemp fiber reinforced PP composite with 5 wt. % MAPP had a 40 %, 70 %, 32 % and 27 % increase in flexural strength and modulus and tensile strength and modulus compared to 15 wt. % hemp fiber reinforced PP composite with 5 wt. % MAPP.
- 30 wt. % hemp fiber reinforced PP composite with 5 wt. % MAPP had a 91 %, 132 %, 122% and 297 % increase, respectively, for the flexural strength and modulus and tensile strength and modulus compared to PP.
- 15 wt. % hemp fiber reinforced PP composite with 5 wt. % MAPP and 30 wt. % hemp fiber reinforced PP composite with 5 wt. % MAPP had the greatest interfacial adhesion due to wetting of the fibers and no apparent gaps between the fiber and matrix after fiber breakage as shown in the SEM images that correlate to the high properties.

Environmental Properties

Fiber treatment and coupling agent additives also improved the flexural, tensile and impact properties of environmentally conditioned 30 wt. % hemp fiber reinforced PP composites. A 20 % decrease in moisture uptake was shown in the accelerated 30 wt. % hemp fiber reinforced PP composite with 5 wt. % MAPP that correlates to the higher flexural and tensile properties compared to the accelerated 30 wt. % untreated hemp fiber reinforced PP composite variance after full saturation. The MAPP addition still had better properties even after being conditioned compared to the 30 wt. % untreated hemp fiber reinforced PP composite variance and had the highest recovery properties of 10-20 %. This recovery indicates that after fiber swelling, there was less damage to the fiber and

fiber interface out of all the variances. In respect to impact strength, a 30 % increase in impact strength after conditioned to full saturation and being re-dried was shown in the 30 wt. % untreated hemp fiber reinforced PP composite and 30 wt. % hemp fiber reinforced PP composite with 5 wt.% NaOH fiber treatment specimens, while only a 15 % increase was shown in the specimens containing MAPP. On the other hand, no significant improvement or decrease in properties was shown when the samples were exposed in a realistic environment of high temperature and humidity

A noticeable decrease in flexural properties was shown after the specimens were exposed to UV radiation for 500 and 1,000 hrs. Fiber exposure and micro-cracking of the matrix were evident in all the samples. 30 wt. % hemp fiber reinforced PP composite with 5 wt. % MAPP samples had the greatest reduction in flexural properties by 30 %, however still had better properties than the 30 wt. % untreated hemp fiber reinforced PP composite and 30 wt. % hemp fiber reinforced PP composite with 5 wt. % NaOH fiber treatment samples.

Duct-Screen Cleaner Prototype

After evaluating the mechanical and environmental properties of 30 wt. % hemp fiber reinforced PP composites, 30 wt. % hemp fiber reinforced PP composite with 5 wt. % MAPP had the best overall results. The use of MAPP means there was no harsh chemical treatment involved with the process that reduces cost, processing time and CO_2 emissions. Long fiber lengths were maintained and minimal moisture uptake was shown in a realistic environment scenario. Through literature understanding and processing and testing evaluation, a successful duct-screen cleaner prototype was optimized and

manufactured. This research proved that it can be correlated to other automotive components and into commercialization. All the research objectives stated earlier have been successfully met with the completion of this thesis.

RECOMMENDATIONS FOR FUTURE WORK

The results obtained during the course of this research through an alternative manufacturing method offers promising future research possibilities. The study findings led to the following recommendations:

- Incorporate a larger scale production since the processing method in this research was lab scale.
- Develop a better understanding of fiber-matrix interface by producing a more accurate mathematical model.
- Analyze and evaluate hybrid natural fiber composites to increase properties for certain automotive components, like incorporating glass fibers or recycled carbon fibers.

LIST OF REFERENCES

[1] B. M. Nzioki, "Biodegradable Polymer Blends and Composites from Proteins Produced by Animal Co-Product Industry," 2010.

[2] J. DeCicco and F. Fung, "Global Warming on the Road: The Climate Impact of America's Automobiles," Environmental Defense, 2006.

[3] SASI Group and Mark Newman, "Fuel Use," 2006. [Online]. Available: http://www.worldmapper.org/posters/worldmapper_map119_ver5.pdf. [Accessed 21 October 2012].

[4] M. A. Brown, F. Southworth and A. Sarzynski, "Shrinking the Carbon Footprint of Metropolitan America," May 2008. [Online]. Available: http://www.brookings.edu/~/media/research/files/reports/2008/5/carbon%20footprint%20sarzynski/carbonfootprint_report.pdf. [Accessed 27 October 2012].

[5] A. Birky, D. Greene, T. Gross, D. Hamilton, K. Heitner, L. Johnson, J. Maples, J. Moore, P. Patterson, S. Plotkin and F. Stodolsky, "Future U.S. Highway Energy Use: A Fifty Year Perspective," 3 May 2001. [Online]. Available: http://www.afdc.energy.gov/pdfs/hwyfuture.pdf. [Accessed 2 November 2012].

[6] J. W. McAuley, "Global Sustainability and Key Needs in Future Automotive Design," *Environmental Science & Technology*, vol. 37, no. 23, pp. 5414-5416, 2003.

[7] U.S. Energy Information Administration, "Annual Energy Outlook 2012 with Projections to 2035," June 2012. [Online]. Available: http://www.eia.gov/forecasts/aeo/pdf/0383(2012).pdf. [Accessed 2 November 2012].

[8] S. Gandhi and R. E. Lyon, "Health Hazards of Combustion Products From Aircraft Composite Materials," U.S. Department of Transportation, Washington, D.C., 1998.

[9] K. Laird, "Green Matter: Evonik launches rayon-reinforced biobased PA," Plastics Today, 17 August 2012. [Online]. Available: http://www.plasticstoday.com/blogs/green-matter-evonik-launches-rayon-reinforced-biobased-pa. [Accessed 2012 November 2012].

[10] Eco-Innovation, "Boosting Green Business," 2011. [Online]. Available: http://ec.europa.eu/environment/eco-innovation/files/docs/publi/eaci_brochure_eco_innovation_a4_lr_en.pdf. [Accessed 16 October 2012].

[11] R. A. Cubeta, "Utilizing Recycled Fiberglass for Affordable, Green Composite Technology," in *COMPOSITES 2013*, Orlando, 2013.

[12] J. Holbery and D. Houston, "Natural-fiber-reinforced polymer composites in automotive applications," *JOM*, vol. 58, no. 11, pp. 80-86, 2006.

[13] G. Beckermann, "Performance of Hemp-Fibre Reinforced Polypropylene Composite Materials," The University of Waikato, New Zealand, 2007.

[14] National Highway Traffic Safety Administration, "Obama Administration Finalizes Historic 54.5 mpg Fuel Efficiency Standards," 28 August 2012. [Online]. Available: http://www.nhtsa.gov/About+NHTSA/Press+Releases/2012/Obama+Administration+Finalizes+Historic+54.5+mpg+Fuel+Efficiency+Standards. [Accessed 21 August 2011].

[15] S. Siler and M. Dushane, "Obama's CAFE Fuel Economy Standards to Create Fleet of Tiny, Expensive Vehicles," May 2009. [Online]. Available: http://www.caranddriver.com/news/obamas-cafe-fuel-economy-standards-to-create-fleet-of-tiny-expensive-vehicles-car-news. [Accessed 22 August 2011].

[16] E. Ghassemieh, "Materials in Automotive Application, State of the Art and Prospects," in *New Trends and Developments in Automotive Industry*, M. Chiaberge, Ed., InTech, 2011, pp. 365-394.

[17] S. Tayabji, K. D. Smith and T. Van Dam, "Advanced High-Performance Materials for Highway Applications: A Report on the State of Technology," Federal Highway Administration, Washington, DC, 2010.

[18] D. B, L. A. Pothan, R. Mavelil-Sam and S. Thomas, "Structure, properties and recyclability of natural fibre reinforced polymer composites," in *Recent Developments in Polymer Recycling*, A. Fainleib and O. Grigoryeva, Eds., India, Transworld Research Network, 2011, pp. 101-120.

[19] R. M. Rowell, D. F. Caulfield and R. E. Jacobson, "Utilization of Natural Fibers in Plastic Composites: Problems and Opportunities," in *Lignocellulosic-Plastics Composites*, Brazil, 1997, pp. 23-51.

[20] D. Verma, P. C. Gope, M. K. Maheshwari and R. K. Sharma, "Bagasse Fiber Composites-A Review," *Journal of Materials and Enviornmental Science*, vol. 3, no. 6, pp. 1079-1092, 2012.

[21] M. Carus, D. Vogt and L. Scholz, "Report on Bio-based Plastics and Composites," April 2010. [Online]. Available: http://www.nova-institut.de/pdf/bwr_april_2010.pdf. [Accessed 23 August 2012].

[22] M. Karus and M. Kaup, "Natural fibres in the European automotive industry," vol. 7, no. 1, pp. 119-131, 2005.

[23] K. Hill, B. Swiecki and J. Cregger, "The Bio-Based Materials Automotive Value Chain," Center for Automotive Research, April 2012. [Online]. Available: http://www.cargroup.org/?module=Publications&event=View&pubID=29. [Accessed 12 August 2012].

[24] K. K. Chawla, Composite Materials: Science and Engineering, 2nd ed., New York: Springer, 1998, pp. 137-42.

[25] A. B. Strong, Fundamentals of Composites Manufacturing: Materials, Methods and Applications, 2nd ed., Dearbon: Society of Manufacturing Engineers, 2008, pp. 1-17.

[26] F. C. Campbell Jr., Manufacturing Processes for Advanced Composites, Oxford: Elsevier Advanced Technology, 2004, pp. 25-31.

[27] P. Tudu, "Processing and Characterization of Natural Fiber Reinforced Polymer Composites," National Institute of Techonology, Rourkela, India, 2009.

[28] S. Mall, "Laminated Polymer Matrix Composites," in *Composites Engineering Handbook*, New York, Marcel Dekker, Inc., 1997, pp. 811-892.

[29] P. K. Mallick, "Random Fiber Composites," in *Composites Engineering Handbook*, New York, Marcel Dekker, Inc., 1997, pp. 893-940.

[30] A. Goel, "Fatigue and Enviornmental Behavior of Long Fiber Thermoplastic (LFT) Composites," The University of Alabama at Birmingham, Birmingham, 2008.

[31] J.-K. Kim and Y.-W. Mai, Engineered Interfaces in Fiber Reinforced Composites, Oxford: Elsevier Science Ltd, 1998.

[32] K. Ilomäki, "Adhesion Between Natural Fibers and Thermosets," Tampere University of Technology, Finland, 2012.

[33] S.-J. Park and M.-K. Seo, Interface Science and Composites, Oxford: Elsevier Ltd., 2011, pp. 659-667.

[34] M. K. A. Arifin, S. Sulaiman, B. H. T. Baharudin, T. S. Hong and S. Sreenivasan, "Simulation of Thermoset Injection for Bulk Moulding Compounds (BMC)," *Key Engineering Materials,* Vols. 471-472, pp. 1101-1106, 2011.

[35] P. C. Painter and M. M. Coleman, Essentials of Polymer Science and Engineering, Lancaster: DEStech Publications, Inc., 2009.

[36] B. D. Agarwal, L. J. Broutman and K. Chandrashekhara, Analysis and Performance of Fiber Composites, Hoboken: John Wiley, 2006.

[37] P. K. Ichhaporia, "Composites from Natural Fibers," North Carolina State University, Raleigh, 2008.

[38] M. D. Beg, "The improvement of interfacial bonding, weathering and recycling of wood fibre reinforced polypropylene composites," The University of Waikto, New Zealand, 2007.

[39] A. E. Dent, C. R. Bowen, R. Stevens, M. G. Cain and M. Stewart, "Tensile strength wood fibre reinforced polypropylene composites," *Ferroelectrics,* vol. 368, pp. 209-215, 2008.

[40] N. Takashi, K. Hirao, M. Kotera, K. Nakamae and H. Inagaki, "Kenaf reinforced biodegradable composite," *Composites Science and Technology,* vol. 63, no. 9, pp. 1281-1286, 2003.

[41] G. N. Onyeagoro and M. E. Enyiegbulam, "Physico-Mechanical Properties of Cellulose Acetate Butyrate/ Yellow Poplar Wood Fiber Composites as a Function of Fiber Aspect Ratio, Fiber Loading, and Fiber Acetylation," *International Journal of Basic and Applied Science,* vol. 1, no. 2, pp. 385-397, 2012.

[42] U. K. Vaidya, A. Goel and K. Chawla, "Fatigue and Vibration Response of Long Fiber Reinforced Thermoplastics," The University of Alabama at Birmingham, Birmingham.

[43] S. I. S. Shaharuddin, M. S. Salit and E. S. Zainudin, "A Review of the Effect of Moulding Parameters on the Performance of Polymeric Composite Injection Moulding," *Turkish Journal of Engineering & Environmental Sciences,* vol. 30, no. 1, pp. 23-34, 2006.

[44] F. L. Matthews and R. D. Rawlings, Composite Materials: Engineering and Science, London: Chapman and Hall, 1994.

[45] S. Taj, A. M. Munawar and S. U. Khan, "Natural fiber-reinforced polymer composites," *Proc. Pakistan Acad. Sci.*, vol. 44, no. 2, pp. 129-144, 2007.

[46] K. v. Rijswijk and W. D. Brouwer, "Application of Natural Fibre Composites in the Development of Rural Societies," Delft University of Technology, Netherlands, 2001.

[47] P. Wambua, J. Ivens and I. Verpoest, "Natural fibres: can they replace glass in fibre reinforced plastics?," *Composites Science and Technology*, vol. 63, no. 9, pp. 1259-1264, 2003.

[48] H. L. Bos, J. A. Van Den Oever and O. C. Peters, "Tensile and compressive properties of flax fibres for natural fibre reinforced composites," *Journal of Materials Science*, vol. 37, no. 8, pp. 1683-1692, 2002.

[49] D. H. Mueller and A. Krobjilowski, "New Discovery in the Properties of Composites Reinforced with Natural Fibers," *Journal of Industrial Textiles*, vol. 33, no. 2, pp. 111-130, 2003.

[50] X. Li, L. G. Tabil and S. Panigrahi, "Chemical Treatments of Natural Fiber for Use in Natural Fiber-Reinforced Composites: A Review," *Journal of Polymers and the Environment*, vol. 15, no. 1, pp. 25-33, 2007.

[51] M. P. Westman, L. S. Fifield, K. L. Simmons, S. G. Laddha and T. A. Kafentzis, "Natural Fiber Composites: A Review," Pacific Northwest National Laboratory, Richland, 2010.

[52] M. Zimmiewska, M. Wladyka-Przybylak and J. Mankowski, "Cellulosic Bast Fibers, Their Structure and Properties Suitable for Composite Applications," in *Cellulose Fibers: Bio-and Nano-Polymer Composites: Green Chemistry and Technology*, London, Springer-Verlag Berlin Heidelberg, 2011, pp. 97-120.

[53] K. Charlet, "Natural Fibres as Composite Reinforcement Materials: Description and New Sources," in *Natural Polymers: Composites*, M. J. John and S. Thomas, Eds., UK, The Royal Society of Chemistry, 2012, pp. 37-57.

[54] J. C. Walker, Primary Wood Processing, Netherlands: Springer, 2006.

[55] G. Siqueira, J. Bras and A. Dufresne, "Cellulosic Bionanocomposites: A Review of Preparation, Properties and Applications," *Polymers*, vol. 2, no. 4, pp. 728-765, 2010.

[56] R. M. Rowell, J. S. Han and J. S. Rowell, "Characterization and factors effecting fiber properties," in *Natural Polymers and Agrofibres Composites*, F. E, L. A and M. H. C, Eds., Brazil, Embrapa Instrumentacao Agropecuaria, 2000, pp. 115-134.

[57] S. J. Eichhorn, C. A. Baillie, L. Y. Mwaikambo, A. Dufresne, K. M. Entwistle, P. J. Herrera-Franco, L. Groom, M. Hughes, T. G. Rials and P. M. Wild, "Current international research into cellulosic fibres and composites," *Journal of Materials Science,* vol. 36, no. 9, pp. 2107-2131, 2001.

[58] L. Donaldson, "Microfibril Angle: Measurement, Variation and Relationships - A Review," *IAWA Journal,* vol. 29, no. 4, pp. 345-386, 2008.

[59] M. J. John and R. D. Anandjiwala, "Recent Developments in Chemical Modification and Characterization of Natural Fiber-reinforced Composites," *Polymer Composites,* vol. 29, no. 2, pp. 187-207, 2008.

[60] L. Y. Mwaikambo, "Review of the History, Properties and Applications of Plant Fibres," *African Journal of Science and Technology,* vol. 7, no. 2, pp. 120-133, 2006.

[61] T. Barman, "Hemp Fibre Composites," 19 December 2011. [Online]. Available: http://www.docstoc.com/docs/108991442/Bombardier_presentation. [Accessed 15 September 2012]

[62] S. Mukhopadhyay, R. Fangueiro, Y. Arpac and U. Senturk, "Banana Fibers-Variability and Fracture Behaviors," *Journal of Engineered Fibers and Fabrics,* vol. 3, no. 2, pp. 39-45, 2008.

[63] M. J. John, R. D. Anandjiwala and S. Thomas, "Lignocellulosic Fibe Reinforced Rubber Composites," in *Natural Fibre Reinforced Polymer Composites: From Macro to Nanoscale,* S. Thomas and L. A. Pthan, Eds., Philadelphia, Old City Publishing, Inc., 2008, pp. 252-266.

[64] A. C. Wibowo, A. K. Mohanty, M. Misra and L. T. Drzal, "Chopped Industrial Hemp Fiber Reinforced Cellulosic Plastic Biocomposites: Thermomechanical and Morphological Properties," *Industrial & Engineering Chemistry Research,* vol. 43, no. 16, pp. 4883-4888, 2004.

[65] M. Pervaiz and M. M. Sain, "Carbon storage potential in natural fiber composites," *Resources, Conservation and Recycling,* vol. 39, no. 4, pp. 325-340, 2003.

[66] E. C. Lee, C. M. Flanigan, K. A. Williams, D. F. Mielewski and D. Q. Houston, "Hemp Fiber Reinforced Sheet Molding Compounds for Automotive Applications," in *SPE Automotive Composites Conference,* Troy, 2005.

[67] Lucintel, "Opportunities in Natural Fiber Composites," March 2011. [Online]. Available: http://www.lucintel.com/LucintelBrief/PotentialofNaturalfibercomposites-Final.pdf. [Accessed 15 September 2012].

[68] S.-J. Kim, J.-B. Moon, G.-H. Kim and C.-S. Ha, "Mechanical properties of polypropylene/natural fiber composites: Comparison of wood fiber and cotton fiber," *Polymer Testing,* vol. 27, no. 7, pp. 801-806, 2008.

[69] E. Ozen, A. Kiziltas, E. E. Kiziltas and D. J. Gardner, "Natural Fiber Blends-filled Engineering Thermoplastic Composites for the Auotmobile Industry," in *SPE ACCE Conference*, Troy, 2012.

[70] S. Georgopoulos, P. A. Tarantili, E. Avgerinos, A. G. Andreopoulos and E. G. Koukios, "Thermoplastic polymers reinforced with fibrous agricultural residues," *Polymer Degradation and Stability,* vol. 90, no. 2, pp. 303-312, 2005.

[71] P. V. Joseph, M. S. Rabello, L. H. Mattoso, K. Joseph and S. Thomas, "Environmental effects on the degradation behaviour of sisal fibre reinforced polypropylene composites," *Composites Science and Technology,* vol. 62, no. 10-11, pp. 1357-1372, 2002.

[72] J. Holbery, L. Fifield, K. Denslow, A. Gutowska and K. Simmons, "Role of Fiber Adhesion in Natural Fiber Composite Processing for Automotive Applications," in *SPE ACCE Conference*, Troy, 2005.

[73] A. Retegi, A. Arbelaiz, P. Alvarez, R. Llano-Ponte, J. Labidi and I. Mondragon, "Effects of hygrothermal ageing on mechanical properties of flax pulps and their polypropylene matrix composites," *Journal of Applied Polymer Science,* vol. 102, no. 4, pp. 3438-3445, 2006.

[74] S. Panthapulakkal and M. Sain, "Studies on the Water Absorption Properties of Short Hemp—Glass Fiber Hybrid Polypropylene Composites," *Journal of Composite Materials,* vol. 41, no. 15, pp. 1871-1883, 2007.

[75] N. A. b. Ahad, N. Parimin, N. Mahmed, S. S. Ibrahim, K. Nizzam and Y. M. Ho, "Effect of Chemical Treatment on the Surface of Natural Fiber," *Journal of Nuclear and Related Technologies,* vol. 6, no. 1, pp. 155-158, 2009.

[76] S. Kalia, B. S. Kaith and I. Kaur, "Pretreatments of Natural Fibers and Their Applications as Reinforcing Material in Polymer Composites - A Review," *Polymer Engineering & Science,* vol. 49, no. 7, pp. 1253-1272, 2009.

[77] N. Suardana, Y. Piao and J. K. Lim, "Mechanical Properties of Hemp Fibers and Hemp/PP Composites: Effects of Chemical Surface Treatment," *Materials Physics and Mechanics,* vol. 11, no. 1, pp. 1-8, 2011.

[78] M. S. Sreekala, M. G. Kumaran, S. Joseph, M. Jacob and S. Thomas, "Oil Palm Fibre Reinforced Phenol Formaldehyde Composites: Influence of Fibre Surface Modifications on the Mechanical Performance," *Applied Composite Materials,* vol. 7, no. 5-6, pp. 295-329, 2000.

[79] I. Ghasemi and M. Farsi, "Interfacial Behaviour of Wood Plastic Composite: Effect of Chemical Treatment on Wood Fibres," *Iranian Polymer Journal*, vol. 19, no. 10, pp. 811-818, 2010.

[80] S. Mishra, J. B. Naik and Y. P. Patil, "The compatibilising effect of maleic anhydride on swelling and mechanical properties of plant-fiber-reinforced novolac composites," *Composites Science and Technology*, vol. 60, no. 9, pp. 1729-1735, 2000.

[81] A. R. Sanadi, D. F. Caulfield, R. E. Jacobson and R. M. Rowell, "Renewable Agricultural Fibers as Reinforcing Fillers in Plastics: Mechanical Properties of Kenaf Fiber-Polypropylene Composites," *Industrial & Engineering Chemistry Research*, vol. 34, no. 5, pp. 1889-1896, 1995.

[82] N. Mfala, "Characterization, Chemical Modification, and Process Optimization of Flax Fiber Natural Composites," The University of Alabama at Birmingham, Birmingham, 2011.

[83] R. Hu and J.-K. Lim, "Fabrication and Mechanical Properties of Completely Biodegradable Hemp Fiber Reinforced Polylactic Acid Composites," *Journal of Composite Materials*, vol. 41, no. 13, pp. 1655-1669, 2007.

[84] A. Thygesen, "Properties of hemp fibre polymer composites - An optimisation of fibre properties using novel defibration methods and fibre characterisation," University of Denmark, Denmark, 2006.

[85] P. C. Struik, S. Amaducci, M. J. Bullard, N. C. Stutterheim, G. Venturi and H. T. Cromack, "Agronomy of fibre hemp (Cannabis sati6a L.) in Europe," *Industrial Crops and Products*, vol. 11, pp. 107-118, 2000.

[86] S. J. Bennett, R. Snell and D. Wright, "Effect of variety, seed rate and time of cutting on fibre yield of dew-retted hemp," *Industrial Crops and Products*, vol. 24, no. 1, pp. 79-86, 2006.

[87] USDA, "Industrial Hemp in the United States: Status and Market Potential," Washinton, D.C., 2000.

[88] N. Said, "The Many Uses of Hemp Part 2," CLEAR, [Online]. Available: http://www.clear-uk.org/the-many-uses-of-hemp-part-2/. [Accessed 15 August 2012].

[89] J. K. Grace, "Termite response to Agricultural fiber composites: Hemp," in *36th Annual Meeting*, India, 2005.

[90] R. Johnson, "Hemp as an Agricultural Commodity," Congressional Research Service, 2013.

[91] M. J. John, K. N. Indira, V. G. Geethamma, J. Shaji and S. Thomas, "Coir and Hemp Fiber-Reinforced Polymer Composites," in *Handbook of Engineering Biopolymers: Homopolymers, Blends and Composites*, S. Fakirov and D. Bhattacharyya, Eds., Munich, Carl Hanser, 2007, pp. 285-307.

[92] K. Hill, B. Swiecki and J. Cregger, "The Bio-Based Materials Automotive Value Chain," Center for Automotive Research, Ann Arbor, 2012.

[93] S. V. Joshi, L. T. Drzal, A. K. Mohanty and S. Arora, "Are natural fiber composites environmentally superior to glass fiber reinforced composites?," *Composites Part A Applied Science and Manufacturing,* vol. 35, pp. 371-376, 2004.

[94] C. D. Rudd, Composites for Automotive Applications, UK: Rapra Technology Limited, 2001.

[95] L. P. Herrera-Estrada, "Processing and Characterization of Banana Fibers and Their Biocomposites," The University of Alabama at Birmingham, Birmingham, 2009.

[96] C. R. Bernal, "Deformation and Fracture Behavior of Natural Fiber Reinforced Polypropylene," in *Polyolefin Composites*, D. Nwabunma and T. Kyu, Eds., Hoboken, John Wiley & Sons, Inc., 2008, pp. 178-201.

[97] Y. Cao, S. Shibata and I. Fukumoto, "Mechanical properties of biodegradable composites reinforced with bagasse fibre before and after alkali treatments," *Composites Part A: Applied Science and Manufacturing*, vol. 37, no. 3, pp. 423-429, 2006.

[98] M. Tajvidi, S. K. Najafi and N. Moteei, "Long-term water uptake behavior of natural fiber/polypropylene composites," *Journal of Applied Polymer Science*, vol. 99, no. 5, pp. 2199-2203, 2006.

[99] M. Huda, L. T. Drzal, D. Ray, A. K. Mohanty and M. Misra, "Natural-fibre composites in the automotive sector," in *Properties and performance of natural-fibre composites*, UK, Woodhead Publishing Limited, 2008, pp. 221-268.

[100] S. Alimuzzaman, R. H. Gong and M. Akonda, "Impact Property of PLA/Flax Nonwoven Biocomposite," in *International Conference on Natural Fibers—Sustainable Materials for Advanced Applications 2013*, Portugal, 2013.

[101] J. Ganster and H. Fink, "Novel cellulose fibre reinforced thermoplastic materials," *Cellulose,* vol. 13, no. 3, pp. 271-280, 2006.

[102] N. Graupner and J. Müssig, "A comparison of the mechanical characteristics of kenaf and lyocell fibre reinforced poly(lactic acid) (PLA) and poly(3-hydroxybutyrate) (PHB) composites," *Composites A,* vol. 42, no. 12, pp. 2010-2019, 2011.